# Chamber investigation of the formation and transformation of secondary organic aerosol in mixtures of biogenic and anthropogenic volatile organic compounds

5 Aristeidis Voliotis[1,*], Mao Du[1,*], Yu Wang[1,*], Yunqi Shao[1,*], M. Rami Alfarra[1,2,‡], Thomas J. Bannan[1], Dawei Hu[1], Kelly L. Pereira[3], Jaqueline F. Hamilton[3], Mattias Hallquist[4], Thomas F. Mentel[5], Gordon McFiggans[1]

[1]Centre for Atmospheric Science, Department of Earth and Environmental Sciences, School of Natural Sciences, University
10 of Manchester, Manchester, M13 9PL, UK

[2]National Centre for Atmospheric Science (NCAS), University of Manchester, Manchester, M13 9PL, UK

[3]Wolfson Atmospheric Chemistry Laboratories, Department of Chemistry, University of York, York, YO10 5DD, UK

[4]Department of Chemistry and Molecular Biology, Atmospheric Science, University of Gothenburg, Gothenburg SE-412 96, Sweden

15 [5]Institut für Energie und Klimaforschung, IEK-8, Forschungszentrum Jülich, Jülich, Germany

‡ now at Environment & Sustainability Center, Qatar Environment & Energy Research Institute, Doha, Qatar

* these authors all made equal contribution to the work and manuscript

*Correspondence to*: Gordon McFiggans (g.mcfiggans@manchester.ac.uk)

**Abstract.** A comprehensive investigation of the photochemical secondary organic aerosol (SOA) formation and transformation
20 in mixtures of anthropogenic (o-cresol) and biogenic (α-pinene and isoprene) volatile organic compound (VOC) precursors in the presence of NOx and inorganic seed particles was conducted. Initial iso-reactivity was used to enable direct comparison across systems, adjusting the initial reactivity of the systems towards the assumed dominant oxidant (OH). Comparing experiments conducted in single precursor systems at various initial reactivity levels (referenced to a nominal base case VOC reactivity) and their binary and ternary mixtures, we show that the molecular interactions from the mixing of the precursors
25 can be investigated and discuss limitations in their interpretation. The observed average SOA yields in descending order were found for the α-pinene (32±7%), α-pinene/o-cresol (28±9%), α-pinene at ½ initial reactivity (21±5%), α-pinene/isoprene (16±1%), α-pinene at ⅓ initial reactivity (15±4%), o-cresol (13±3%), α-pinene/o-cresol/isoprene (11±4%), o-cresol at ½ initial reactivity (11±3%), o-cresol/isoprene (6±2%) and isoprene systems (0±0%). We find a clear suppression of the SOA yield

Atmospheric
Chemistry
and Physics
Discussions

from α-pinene when it is mixed with isoprene, whilst the addition of isoprene to o-cresol may enhance the mixture's SOA

30    formation potential, however, the difference was too small to be unequivocal. The α-pinene/o-cresol system yield appeared to be increased compared to that calculated based on the additivity, whilst in the α-pinene/o-cresol/isoprene system the measured and predicted yield were comparable. However, in mixtures where more than one precursor contributes to the SOA mass it is unclear whether changes in the SOA formation potential are attributable to physical or chemical interactions, since the reference basis for the comparison is complex. Online and offline chemical composition and SOA particle volatility, water

35    uptake and "phase" behaviour measurements that were used to interpret the SOA formation and behaviour are introduced and detailed elsewhere.


## 1.    Introduction

The fine fraction of particulate matter (PM) plays the dominant role in the impact of air pollution on human health and of

40    aerosol on climate through direct radiative effects and cloud adjustments. Ambient $PM_{2.5}$ was the fifth-ranking global mortality risk factor in 2015, with exposure to it causing 4.2 million deaths and 103.1 million disability-adjusted life-years (DALYs), 7.6% of total global deaths and 4.2% of global DALYs (Cohen et al., 2017). Moreover, fine PM is responsible for the aerosol effects that make the single greatest contributory uncertainty to radiative forcing (IPCC, 2013).

Organic material makes a major contribution to the mass of fine PM in the atmosphere (Jimenez et al., 2009) and secondary

45    organic aerosol (SOA) is the major contributor (Hallquist et al., 2009). Nonetheless, our ability to predict the atmospheric burden and hence impacts of fine secondary aerosol particles (Kanakidou et al., 2005; Tsigaridis and Kanakidou, 2018) has been limited by basic understanding of the formation of this organic component (Hallquist et al., 2009). Photochemistry dictates the levels of $NO_2$, $O_3$ and the SOA fraction of PM. Whilst it is relatively straightforward to understand and control primary pollutants, these secondary pollutants make a substantial contribution to air quality degradation that are set to become

50    increasingly important as primary pollutants are cleaned up. However, understanding the rate and extent of SOA formation in the real atmosphere presents a number of challenges. There are tens of thousands of isolated organic compounds in the atmosphere, ranging across more than 12 orders of magnitude in volatility (Goldstein and Galbally, 2007) with possible oxidation products running to many millions (Aumont et al., 2005). They have extensive biogenic and anthropogenic sources and are spatially heterogeneous. Their reactivity ranges over many orders of magnitude and their lifetimes at ambient oxidant

55    levels consequently range from less than a second to several years. An unknown but substantial proportion of the organic compounds have the potential to act as SOA precursors and the degree to which this is influenced by the complex atmospheric mixture is unclear.

It has long been established that prediction of the formation of secondary gaseous pollutants in the troposphere requires knowledge of the nature of the mixture of volatile organic compounds (VOC), their abundance and the chemical regime (e.g.

Atmospheric
Chemistry
and Physics
Discussions

60   VOC : NO$_x$ ratio) and airmass history. In contrast, the formation of SOA in the real atmosphere is conventionally considered less mechanistically. Against the backdrop of the near unimaginable complexity of the atmospheric mixture of SOA precursors, the basis for our understanding of SOA formation has been primarily derived from experimental investigations of single component systems (Thornton et al., 2020; Donahue et al., 2012; Jenkin et al., 2012). A wealth of literature derived from chamber experiments on biogenic (Thornton et al., 2020; Carlton et al., 2009) and anthropogenic (Schwantes et al., 2017;

65   Nakao et al., 2012) precursors under a range of chemical environments combined with fundamental kinetic studies (Ziemann and Atkinson, 2012; Cash et al., 2016) has enabled numerous representations of atmospheric SOA at varying levels of detail (Shrivastava et al., 2017; Charan et al., 2019). There have additionally been studies of SOA formation in source-oriented mixtures from diesel (Weitkamp et al., 2007; Nakao et al., 2011) and gasoline (Nordin et al., 2013; Platt et al., 2013) exhaust, woodburning (Tiitta et al., 2016), cooking (Reyes-Villegas et al., 2018; Kaltsonoudis et al., 2017) and from macroalgal

70   (McFiggans et al., 2004) and plant (Joutsensaari et al., 2005; VanReken et al., 2006; Pinto et al., 2007; Mentel et al., 2009; Hao et al., 2009; Wyche et al., 2014) emissions. Building on a well-established framework first suggested by Pankow (1994) to account for absorptive partitioning of mixtures of organic components in the atmosphere, attempts have been made to provide empirically constrained and mechanistically augmented conceptual frameworks of organic aerosol (Donahue et al., 2006; Donahue et al., 2011; Schervish and Donahue, 2020), but there is currently no universally accepted mechanistic basis

75   for SOA understanding in the complex atmosphere.

Evidence suggests that it is necessary to take a more mechanistic approach in order to capture observed behaviour of SOA formation in mixtures. It was established that the scavenging of the OH radical by addition of isoprene significantly inhibits new particle formation in plant chamber studies (Kiendler-Scharr et al., 2009), though the atmospheric implication was questioned by Berndt et al. (2018) since OH will likely not be controlled by isoprene. More recent studies have indicated that

80   the mass and yield of SOA formed from individual precursors may similarly be influenced by the presence of other VOC (McFiggans et al., 2019). In addition to the observed suppression of particle mass and yield from $\alpha$-pinene being attributed to the established scavenging of oxidant by the lower SOA yield isoprene, it was found that the C$_5$ peroxy radical isoprene oxidation products scavenged highly oxygenated C$_{10}$ peroxy radicals that would otherwise form extremely low volatility condensable compounds. This had also been reported by Berndt et al. (2018) who demonstrated a similar scavenging of C$_{10}$

85   radical products in the presence of ethylene. McFiggans et al. (2019) further reported such product scavenging and consequent reduction in $\alpha$-pinene SOA yield by CO and CH$_4$. Such interactions should be no surprise, given our understanding of peroxy radical cross reactions and termination fates in controlling production of secondary gaseous pollutants. Moreover, the existence of such interactions in mixtures is somewhat obvious in the light of the understanding that has emerged over recent years (e.g., Bianchi et al., 2019) of the roles of atmospheric autoxidation of VOC producing highly oxygenated organic molecules (HOM).

90   Following the early postulations of the role of autoxidation in atmospheric VOC degradation (Crounse et al., 2013), the importance of HOM in SOA formation has been widely established and quantified in monoterpene oxidation (Ehn et al., 2012; Ehn et al., 2014; Jokinen et al., 2015; Berndt et al., 2016; Berndt et al., 2018; Bianchi et al., 2019). The termination of the RO$_2$

formed via autoxidation ("HOM-RO$_2$") will depend on the chemical conditions (the abundance of NO$_x$, HO$_2$ and the numerous other RO$_2$ species present in the mixture) as well as the formation rate of the HOM-RO$_2$. Schervish and Donahue (2020) provide a discussion of the determinants of the fate of HOM-RO$_2$ and potential consequences on the distribution of low, extremely low and ultra-low volatility organic compound (LVOC, ELVOC and ULVOC respectively) products and hence on SOA formation in $\alpha$-pinene oxidation. Autoxidation is widespread and common and, in atmospheric systems, is unlikely to be restricted to monoterpenes (though unsaturated compounds may be expected to be more susceptible). Indeed, the application of recently developed mass spectrometric techniques has revealed the presence of HOM in the oxidation of aromatic compounds (Wang et al., 2017; Wang et al., 2020; Molteni et al., 2018; Tsiligiannis et al., 2019; Garmash et al., 2020; Mehra et al., 2020; Priestley et al., 2021). The degree to which the HOM distribution results from direct autoxidation or from multigenerational pathways is unclear, though the prevalence of HOM-RO$_2$ during aromatic oxidation is clear. The attention on aromatic compounds has been driven by their relevance as anthropogenic VOC emissions, making significant manmade contributions to the VOC burden in the polluted troposphere. Given the prevalence and diversity of autoxidation mechanisms, it is probable that HOM would be detected on the application of modern mass spectrometry to the investigation of many classes of atmospheric VOC. The recent focus on interactions via autoxidation in mixtures has added to more well-established mechanistic linkages in the oxidation of VOCs for understanding gas phase photochemistry. The implications on production of aerosol particle precursors are less well studied. Since the fractional contribution of HOM to particle mass is unclear, the role of autoxidation and influences of interactions on the HOM contributions to SOA mass formation in mixtures is unquantified. It is therefore important to additionally maintain a focus on influences of the non-HOM components on SOA formation in oxidation of VOC mixtures.

Given the potential diversity in VOC sources contributing to the pollutant mixture in the ambient atmosphere, it is important to establish the experimental basis for an understanding of SOA formation beyond the recently studied "simple" biogenic mixed systems (Berndt et al., 2018; McFiggans et al., 2019; Shilling et al., 2019). The importance of establishing a framework to understand interactions in systems of mixed anthropogenic and biogenic VOC stretches well beyond speculative curiosity. Such a framework may be a key to explaining observed non-linearities when natural and manmade pollution mixes (Spracklen et al., 2011; Emanuelsson et al., 2013). Using such considerations as motivation, a series of experiments was conceived to explore SOA formation from typical biogenic and anthropogenic VOC precursors and their binary and ternary mixtures. The binary $\alpha$-pinene/isoprene system reported elsewhere was used as a biogenic mixture with established mechanistic interactions in its photo-oxidation. $o$-cresol was chosen as a representative anthropogenic VOC, being both emitted as a primary pollutant and formed through oxidation of other aromatic compounds. The construction of the study is detailed in the methodology section below. The experiments were conducted in the 18m$^3$ Manchester Aerosol Chamber (MAC), a photochemical chamber operating in batch mode. The design of experiments on mixed VOCs is complex and requires consideration of aspects not encountered in single VOC experiments. This paper explores many of these elements and associated challenges with a view to inform best practice in their planning and executions. The objectives were broad and diverse and aimed to:

4

Atmospheric
Chemistry
and Physics
Discussions

i) establish the suitability of the experimental design for investigating SOA formation in VOC mixtures;

ii) establish the suitability of conventionally reported metrics such as SOA mass yield for quantifying SOA formation in VOC mixtures;

iii) using these metrics, quantify any interactions in VOC mixtures leading to changes in the SOA formation from that may be
130    expected based on single precursor experiments;

iv) using a suite of online and offline measurements of chemical and physical properties, to probe the chemistry and physics leading to these interactions and the properties of particles resulting from them, of potential atmospheric significance.

This paper will address the first three of these and provide an introduction to the findings related to the fourth, which will be detailed in a number of companion manuscripts. It is envisaged that the programme will act as a springboard to investigate the
135    detailed mechanisms of interactions in mixtures of VOC involved in ambient SOA formation.

Importantly, this paper aims to explore whether SOA experiments using multiple VOC precursors can reveal aspects of the multiphase atmospheric systems inaccessible to experiments using a single precursor species.

## 2.    Experimental design

140    The mixture of atmospheric VOCs and variability in prevailing oxidising environment is so complex that the choice of precursors, concentrations and experimental conditions makes a comprehensive programme intractable. Besides challenges associated with representativeness of atmospheric complexity and concentrations in the multiphase system, numerous infrastructural considerations and measurement challenges must be considered. There are additional conflicts in the requirements needed to fully address specific objectives of the study. In this section, these criteria and the bounds placed on
145    the study are addressed and the approaches to experimental design in response to these restrictions and requirements are discussed along with the choices made. Finally, the capabilities and likely consequences and compromises inherent in these choices are listed, before outlining the methodology employed.

### 2.1. VOC mixture and oxidant "representativeness"

Of the tens of thousands (or perhaps millions) of atmospheric organic compounds present in the vapour phase, only a handful
150    have been studied in previous chamber SOA experiments and fewer in mixtures. The selection of compounds for the study of mixed SOA precursors is simultaneously simple and complex; simple, insofar as study of a random mixture will yield novel results, but complex, in that care is required to maximise their importance. Disregarding chlorine atoms and the Criegee radicals

as "exotic", the dominant oxidants at night are the nitrate radical ($NO_3$) and ozone and during the day, the hydroxyl radical (OH) and ozone. Whilst arguments (such as likely / possible dominance of daytime oxidising capacity and pathways to SOA

155    over night-time) can be used to select the oxidant combination of interest, this is fairly arbitrary and open, and we have selected daytime oxidation conditions for the present study.

Similarly arbitrary is the selection of $NO_x$ regime. Whilst VOC:$NO_x$ ratio dependence of SOA formation from some precursors has been well studied (e.g. Pullinen et al. 2020), this is not the case for mixtures of VOC. It is established for certain systems that SOA formation pathways in low and high $NO_x$ regimes change dramatically and consequently influence SOA particle

160    mass yield (e.g. Sarrafzadeh et al. 2016). Challenges associated with the comparability of experimental configurations and conditions lead to apparently conflicting findings and controversies remain surrounding the influence of NOx on SOA formation, requiring unambiguous mechanistic resolution. Truly low $NO_x$ regimes probably do not occur widely in the ambient atmosphere, at least not in the perturbed northern hemisphere. Moreover, in light of selection (see below) of an anthropogenic SOA precursor in the mixture, it would be unreasonable to expect there to be a complete absence of $NO_x$. For reasons outlined

165    below (sections 2.4 and 2.5) related to the chosen concentrations and contributions to reactivity, this study uses moderate VOC:$NO_x$ ratios (between roughly 3 and 8) broadly corresponding to a perturbed background chemical regime.

The reactivity of gaseous VOCs towards ambient oxidants spans several orders of magnitude and the ratio of reactivity towards each oxidant varies substantially. In particular, reactivity towards ozone will be negligible for saturated VOCs but can lead to lifetimes of a few minutes for reactive sesquiterpenes. In order for each VOC in a mixture to contribute significantly to the

170    distribution of oxidation products in a chamber experiment and thereby influence the pathways to, and potential for, SOA formation, it is desirable for them to have comparable reactivity towards the available oxidants. In such a mixture, similar concentrations of each VOC might be reasonably expected to provide a comparable rate of change of oxidation products into the mix and hence contribute to SOA production pathways. Our approach to this is outlined in section 2.4.

As with reactivity, the SOA particle formation potential of VOCs can vary widely, from unmeasurably low to having particle

175    mass yields of several tens of percent. Intuitively, the presence of a higher yield VOC might be expected to contribute more mass than a lower yield VOC and consequently increase the yield of the mixture. What is less clear is the degree to which a lower yield component might reduce the yields of a higher yield VOC and vice versa – i.e. how strongly is the chemistry coupled and how do such interactions influence SOA particle formation? More fundamentally, the reference for and calculation of yields in VOC mixtures is a challenge depending on the often arbitrary selected definition (see results and discussion sections

180    4 and 5).

A final consideration is the sort of atmosphere that the experiment aims to represent. McFiggans et al (2019), in their choice of α-pinene and isoprene, have looked at binary mixtures of abundant biogenically-emitted VOCs (as did Jaoui and Kamens, 2003, previously, in looking at mixtures of α- and β-pinene). Much of the global atmosphere is perturbed by anthropogenic

pollutants and contributions from natural and manmade sources at any location or time will depend upon the mixture and

185 strength of, and distance from, upwind sources (amongst a multitude of other factors). This study builds on previous insight from the binary mixture of low and high yield biogenic SOA precursors to add a moderate yield anthropogenic VOC. Studies could equally be focused on a range of high, low or moderate SOA yield manmade VOCs or numerous other combinations. Indeed, such extension and broadening of the current approach will be of substantial interest.

## 2.2. Infrastructural and instrumentational considerations

190 This study employs a mixture of VOCs as SOA precursors – i.e. compounds almost entirely in the vapour phase under normal temperate surface atmospheric conditions. This straightforwardly takes advantage of the heated glass bulb arrangement in the MAC for the injection of small amounts of liquid organic components and enables comparability with other studies using conventional SOA precursors. Future work could readily use materials from solid stock for studies of "unconventional" SOA precursors that have had much recent attention, such as those falling into the intermediate volatility (IVOC) and semi-volatile

195 (SVOC) classes.

All experiments employed ammonium sulphate seed particles. This was primarily to enable greater reproducibility by providing sufficient particulate mass to act as a condensation sink for partitioning compounds, suppressing nucleation and its attendant stochastic elements. In chamber experiments, there is a competition for condensable vapours between the walls and any existing particles such that seeded experiments enable earlier formation of SOA particle mass. Moreover, detection of this

200 particle mass, and determination of their composition and properties is more straightforward with instruments that require particles to be greater than a certain size. Whilst we previously pioneered the technique of generation of SOA particle seeds for use in chamber experiments (Hamilton et al., 2011), use of ammonium sulphate avoids the additional complication of the chemistry by residual VOC oxidation products. Ammonium sulphate is nebulised into a stainless-steel retaining drum prior to entrainment into the final fill cycle for the experiment (see methods section 3, below). It is recognised that inorganic seeds

205 may not present the most effective absorptive medium for condensational uptake of organic vapours, but the seed generation process is highly reproducible and an implicit assumption of the likelihood of comparable efficiency as an absorptive medium across the systems of choice is made. Acidic seeds are not accessible in the MAC, because uptake of background ambient $NH_3$ leads to neutralisation of $H^+$ at any reasonable seed mass loading.

Instrumental detection limits and sampling requirements dictate the accessible range of concentrations for the experiments (see

210 table 2). State-of-the-science sampling and measurement techniques are employed throughout. Many are capable of very high precision and time resolution measurement at low concentrations. Some are capable of single particle detection or particle ensemble measurement by number concentration. Most of the approaches employ online, or semi-continuous, operation and low concentrations could be readily accommodated by increasing instrument integration times. Filters are collected for molecular determination of SOA particle composition by the evacuation of the entire chamber through pre-fired quartz filters

215 (section 3). Collection of sufficient mass provides a lower limit to the mass concentration loadings and dictates moderately high injected VOC concentration (dependent on the particle mass yield of the mixture). The consequences of higher-than-ambient VOC and PM mass loadings are discussed in section 5.

Very low $NO_x$ studies are not accessible in the MAC, owing to variable and sometimes elevated $NO_x$ concentrations in our chamber laboratory in the centre of Manchester. Such conditions limit the ability of our Purafil scrubber to completely remove

220 $NO_x$ at our high inlet flow and may potentially lead to the increase in $NO_x$ by diffusion through the Teflon film. Such effects would be non-negligible when attempting sub-ppbv $NO_x$ experiments but present modest challenges at higher $NO_x$ conditions, unnoticeable under the chosen VOC concentrations and moderate VOC:$NO_x$ ratios of the current programme.

The chemical conditions in all experiments were controlled by photo-oxidation under a simulated solar spectrum at moderate VOC:$NO_x$ ratio, with $NO_x$ injected as $NO_2$. In all experiments, neutral ammonium sulphate was injected to provide a

225 condensation sink sufficiently large to compete effectively with the wall for condensable vapours. Table 1 shows the initial conditions of all experiments.

### 2.3. Ideal, desirable and realistic objectives

It is not the intention to quantitatively establish the extent and nature of interactions between VOC precursors in the

230 photochemical processes leading to SOA particle formation in ambient mixtures and the consequent impacts on SOA composition and properties in the real atmosphere. The VOC mixtures and set of experimental conditions is a small sample across a large chemical and physical space. The current programme aims to reveal examples of the behaviours in mixed systems and provide indicative quantifications of potential interactions and consequences. A focus is placed on the physical properties and chemical composition of the evolving particle distribution throughout the photochemistry driving its formation and

235 transformation. Less emphasis is placed on the quantification of the radical chemistry and oxidative environment although some characterisation of the transformations of the oxidation products in the gas phase and their influence on the particle formation is attempted. The experimental design and instrumentational payload are used so far as possible to contribute to addressing the objectives outlined in section 1.

240

Atmospheric
Chemistry
and Physics
Discussions

**Table 1:** List of initial experimental conditions for all the experiments in the campaign.

| Exp. No | Exp. Type | VOC | NOx (ppb) | VOC (ppb)[a] | VOC/NOx (ppb/ppb) | Seed (μg m⁻³) | SOA mass (μg m⁻³) |
|---|---|---|---|---|---|---|---|
| | Single | | | | | | |
| 1 | | α-pinene | 40 | 309 | 7.7 | 72.6 | 273.2 |
| 2 | | α-pinene | 43 | 309 | 7.2 | 67.6 | 283.1 |
| 3 | | α-pinene | 50 | 309 | 6.2 | 39.4 | - |
| 4 | | α-pinene | 26 | 155 | 6.0 | 45.7 | 68.6 |
| 5 | | α-pinene | 35 | 155 | 4.4 | 47.8 | 109.5 |
| 6 | | α-pinene | 18 | 103 | 5.7 | 51.0 | 31.5 |
| 7 | | o-cresol | 98 | 400 | 4.1 | 50.8 | 28.2 |
| 8 | | o-cresol | 44 | 400 | 9.1 | 47.8 | 56.0 |
| 9 | | o-cresol | 71 | 400 | 5.6 | 36.0 | - |
| 10 | | o-cresol | 40 | 200 | 5.0 | 51.3 | 22.8 |
| 11 | | isoprene | 24 | 164 | 6.8 | 64.1 | 0.0 |
| 12 | | isoprene | 23 | 164 | 7.1 | 101.9 | 0.0 |
| 13 | | isoprene | 14 | 55 | 3.9 | 42.2 | 0.0 |
| | Binary | | | | | | |
| 14 | | o-cresol/isoprene | 34 | 282 (200/82) | 8.3 | 49.6 | 11.2 |
| 15 | | o-cresol/isoprene | - | 282 (200/82) | - | 57.0 | 9.4 |
| 16 | | α-pinene/o-cresol | 52 | 355 (155/200) | 6.8 | 48.3 | 122.3 |
| 17 | | α-pinene/o-cresol | 65 | 355 (155/200) | 5.5 | 72.9 | - |
| 18 | | α-pinene/o-cresol | - | 355 (155/200) | - | 42.5 | 130.1 |
| 19 | | α-pinene/isoprene | 33 | 237 (155/82) | 7.2 | 63.7 | 96.6 |
| 20 | | α-pinene/isoprene | 39 | 237 (155/82) | 6.1 | 62.0 | 100.9 |
| 21 | | α-pinene/isoprene | 24 | 237 (155/82) | 9.9 | 50.5 | 75.2 |
| | Ternary | | | | | | |
| 22 | | α-pinene/o-cresol/isoprene | 80 | 291 (103/133/55) | 3.6 | 45.6 | 55.5 |
| 23 | | α-pinene/o-cresol/isoprene | 60 | 291 (103/133/55) | 4.9 | 49.0 | 51.4 |
| 24 | | α-pinene/o-cresol/isoprene | 78 | 291 (103/133/55) | 3.7 | 45.8 | 58.0 |

[a]All nominal reported initial VOC concentrations have a ± 15% measurement uncertainty. The individual VOC concentration

245   in the binary and ternary mixtures shown in brackets correspond to the precursor VOC listing. A dash indicates missing data

owing to instrument problems.

### 2.4. Concept behind the experimental design

250 Taking into account the constraints and challenges outlined above, the programme was constructed to investigate a single ternary system comprising one anthropogenic and two biogenic VOCs. The biogenic VOCs were chosen as $\alpha$-pinene and isoprene to enable comparison of batch reactor experiments with previous flowtube (Berndt et al., 2018), well-mixed continuously stirred tank reactor (McFiggans et al., 2019) or flow-through chamber studies (Shilling et al., 2019). The anthropogenic aromatic OVOC $o$-cresol was chosen for its fairly rapid rate constant with OH ($4.1 \times 10^{-11}$ cm$^3$molec$^{-1}$s$^{-1}$), such

255 that it would exhibit comparable reactivity towards OH as a similar concentration of $\alpha$-pinene or isoprene. A concept of "initial isoreactivity" towards OH was employed to select ratios of the initial concentrations of the VOCs. This meant that the initial mixing ratios were injected at an $\alpha$-pinene : isoprene : $o$-cresol ratio of 309 : 164 : 400 based on the ratios of the inverse of their IUPAC-recommended rate constants at 298K (Atkinson et al., 2006; Mellouki et al., 2021). In order to construct a systematic investigation of the single precursor, binary and ternary mixtures, individual VOC experiments were conducted at

260 full-, half- and third-reactivity for comparison of SOA particle mass, composition and properties. Using previously reported values for the SOA particle mass yields, it was expected that an initial full-reactivity mixing ratio in the 100s ppbv range would provide the 10 to a few 100 μgm$^{-3}$ required to provide enough particle mass on the filter at the end of an experiment (at a final chamber volume of around 10 m$^3$) for molecular characterisation.

### 2.5. Compromises in the experimental plan and consequences

265

OH is only one of the likely oxidants under the chosen photo-oxidation conditions, and the unsaturated biogenic compounds will each react with ozone with appreciable reactivity. $o$-cresol exhibits negligible reactivity towards ozone. Ozone is the first oxidant to be formed through photolysis of NO$_2$, and there will be appreciable formation of biogenic oxidation products prior to formation of those from $o$-cresol (see section 4).

270 In addition to the differential reactivity towards the two dominant oxidants, there will be differences in the product formation rates in the single VOC experiments with varying concentrations owing to the use of a single VOC:NOx ratio. This will result from the reduced NO$_x$ at reduced VOC, which will lead to reduced OH concentration owing to reduction in the NO + HO$_2$ flux. Though there will also be a reduced rate of production of ozone in these experiments, non-linearity will lead to changes in the O$_3$: OH ratio and hence changes in the contributions of the oxidation pathways for the biogenic VOCs. There may be

275 less expected influence on the pathways for $o$-cresol oxidation, though the rate of oxidation will nevertheless be slowed.

Ambient atmospheric OH reactivity can be estimated from the quantification of VOC abundance or from direct measurements of OH lifetime. Using the latter, Whalley et al. (2016) reported central London diurnal average morning peaks of around 27 s$^{-1}$ and a campaign maximum of around 116 s$^{-1}$. Our full reactivity experiments have an OH reactivity around 465 s$^{-1}$, some 4

times higher with only one, two or three VOCs for single precursor, binary or ternary experiments respectively. It would be
desirable to work with lower concentrations. In addition to challenges associated with maintaining oxidant levels at such high
VOC concentrations, there is likelihood that the chemical regime, particularly with respect to radical concentrations may
introduce biases in observed system behaviour. In our systems, OH reactivity is provided by $C_5$, $C_7$ and $C_{10}$ VOC compounds
(in addition to that provided by $NO_2$ and VOC oxidation products formed by the oxidation). This will lead to a high abundance
of relatively large peroxy-radical, $RO_2$, species. OH reactivity in the ambient atmosphere is likely to be distributed amongst a
high diversity of small (including CO and $CH_4$) and larger components (including carbonyls and other oxygenates). The
distribution of $RO_2$ and the ratio of $RO_2 : HO_2$ may be substantially different. Nonetheless, it is not the intention or objective
of the current study to mimic the atmospheric chemical regime, more to explore the potential for mixed VOC systems to reveal
interactions in SOA formation processes.

A further consideration is the selection of neutral seed experiments. The systems studied will more reflect direct partitioning
of gaseous oxidation products rather than accounting for products of condensed phase, particularly acid catalysed, reactions.
Again, the intention is not to comprehensively mimic the atmosphere and this is recognised in the interpretation and discussed
in further detail in section 5.

### 3. Methodology

All experiments were performed in the MAC; a 18$m^3$ FEP Teflon bag mounted on three pairs of rectangular extruded
aluminium frames and housed in an air-conditioned enclosure. In the MAC, ground-level solar illumination is simulated using
two 6 kW Xenon arc lamps and a bank of halogen lamps, mounted on the inner aluminium wall of the enclosure which is lined
with reflective "space blanket" material to maximise and homogenise the light intensity across the chamber.  Removal of
unwanted heat from the lamps is provided by the temperature and RH conditioned air introduced between the bag and the
enclosure at 3 $m^3$ $s^{-1}$ and active water cooling of the mounting bars of the halogen lamps and of the filter in front of the arc
lamps. In addition to removing the heat from the arc lamp, the water in the filters removes unwanted IR radiation and the 4mm
quartz plates forming the filter windows remove all UV radiation below 290 nm and increasingly transmit light up to a 100%
transmission above 305 nm. The inlet comprises a high flowrate blower, feeding dried laboratory air through 50 mm diameter
stainless steel pipework to a series of high-capacity filters and variously via a series of two- and three-way electropneumatic
valves to a humidifier, ozoniser and aerosol generation drum before delivering it to the chamber through a Teflon manifold.
This is mounted on the top frame of the central rigidly fixed pair of frames. The upper and lower pairs of frames are counter-
weighted and free to track vertically, allowing the bag to expand and collapse as it is filled and flushed, by switching the valve
positioning.

All controls are automated, and a series of pre- and post-experimental procedures have been programmed, comprising
310   repeatable, characterised sequences of filling and flushing. The pre-experiment sequence is conducted prior to each experiment
to ensure an adequately low background of indicative particulate and gaseous contaminants, monitored by CPC, $NO_x$ and $O_3$
analysers. A one-hour long chamber background characterisation procedure, following the pre-experiment sequence, is
conducted to ensure that a baseline contamination level has been established. This is followed by injection of the VOCs, $NO_x$
and seed particles and a one-hour collection of data from the experimental background in the dark, during which the chamber
315   conditions and all instrumentation are stabilised.  A post-experiment sequence is conducted after each experiment to flush the
chamber of all residual contaminants and leave a clean bag for the next experiment. The final fill of the post-experiment
sequence contains ppm levels of ozone which is used to soak the chamber overnight between subsequent experiments. A
weekly vigorous clean is conducted with full illumination with no UV filter on the arc lamps and ppm levels of ozone at high
RH for maximum OH production.

320   Ammonium sulphate seed particles are atomised into a 50L stainless steel drum for pre-concentration prior to injection into
the chamber.  The seed concentration in the chamber is controlled by altering the injection time into the drum and the
concentration of the stock solution (0.01 g/ml). After the final pre-experiment flush cycle, the fill flow is diverted through the
drum. Liquid α-pinene, isoprene and $o$-cresol are injected as required through the septum of a heated glass bulb and evaporated
into an $N_2$ carrier flow into this final fill along with $NO_x$ as $NO_2$ from a cylinder, also carried by $N_2$. Photochemistry is initiated
325   by irradiating the VOC at moderate VOC / $NO_x$ ratio using the lamps as described above. Online instrumentation is used to
continuously monitor the concentration of $NO_x$, $O_3$, particle number and mass throughout each experiment. It should be noted
that $o$-cresol was found to interfere with $O_3$ measurement as a result of its UV absorption. The decay of CIMS-measured $o$-
cresol was used to correct the $O_3$ data in all $o$-cresol containing experiments. The dark $o$-cresol measured before introduction
of $O_3$ into the MAC was used to calibrate the $O_3$ analyser signal for absorption by $o$-cresol. The decay rate of the CIMS $o$-
330   cresol signal was used to correct the $O_3$ measurements during the experiment. It should be noted that any UV absorption from
the oxidation products of $o$-cresol cannot be captured and $O_3$ is thus reported as an upper limit in $o$-cresol containing systems.

335

**Table 2:** List of instrumentation employed over the course of the study

| Instrument | Model | Measured parameter | LOD/ range |
|---|---|---|---|
| Dew point hygrometer | Edgetech (DM-C1-DS2-MH-13) | Dew point | -20 – 90 ± 0.2 °C |
| NOx analyser | Thermo 42i | NO, NO$_2$ | 0.5 to 1000 ppb |
| O$_3$ analyser | Thermo 49C | O$_3$ | 0-0.05 to 200 ppm |
| Water.based condensation particle counter | TSI 3786 | Particle number | <10$^7$ p/cc |
| Differential mobility particle sizer | Custom.built[a] | Particle size | 40-600 nm |
| Filter collector | Custom.built[b] | Particle collection for offline analysis | |
| Condensation particle counter | TSI 3776 | Particle number | <10$^7$ p/cc |
| Scanning mobility particle sizer | TSI 3081 | Particle size | 10-1000 nm |
| High-resolution aerosol mass spectrometer | Aerodyne | PM$_1$ non.refractory particle composition | >0.05 μg m$^{-3}$ |
| Iodide chemical ionisation mass spectrometer | Aerodyne/Tofware | Oxygenated VOC | LOD >60 ppt; Mass resolution 4000 Th/Th |
| Filter Inlet for Gases and AEROsols | Aerodyne/Tofware | Particle composition | >10$^2$ ng |
| Semi-continuous gas-chromatograph mass spectrometer | 6850 and 5975C Agilent | VOC concentration | >0.4 ppb |
| Liquid chromatograph – orbitrap mass spectrometery | Dionex 3000, Orbitrap QExactive, ThermoFisher Scientific | Particle composition | |
| Hygroscopicity tandem differential mobility analyser | Custom.built[c] | Hygroscopicity | 20-350 nm |
| Cloud condensation nuclei counter | Droplet measurement Tech (model CCN-100) | CCN activity | >6 x 10$^3$ particles cm$^{-3}$ at SS:0.2% |
| Thermal denuder | Custom.built[d] | Volatility | Temperature range: ambient – 200°C |
| Three arm bounce impactor | Custom.built[e] | Particle bounce | 20-500 nm, < 10$^4$ particles cm$^3$ |

[a]Alfarra et al. (2012)
[b]Hamilton et al. (2011)
[c]Good et al. (2010)
[d]Voliotis et al. (2021a)
[e]Liu et al. (2017)

340

Atmospheric
Chemistry
and Physics
Discussions

Open Access
EGU

345    A high-resolution time-of-flight Aerosol Mass Spectrometer (HR-ToF-AMS; Aerodyne Inc.) is used to measure particle composition by mass, a Filter Inlet for Gases and Aerosols coupled to an iodide chemical ionisation mass spectrometer (FIGAERO-I⁻-CIMS; Aerodyne Inc.) for gas and particle phase oxygenated component measurement, a scanning mobility particle sizer (SMPS; TSI Inc.) for particle size distribution retrieval, a home-built hygroscopicity tandem differential mobility analyser (HTDMA) for hygroscopic growth factor determination, a cloud condensation nucleus counter (CCNc; DMT Inc.)

350    for cloud droplet potential evaluation and a home-built three arm bounce impactor for particle rebound determination. Some of the online instrumentation was switched after several hours to cycle between sampling after a home-built thermodenuder (TD) and directly from the chamber. Finally, a semi-continuous 2-trap Gas Chromatograph with Mass Spectrometric detection (GC-MS; Agilent) was used to monitor VOC concentrations. Table 2 provides a list of all instrumentation employed throughout the programme. At the end of each 6-hour experiment, the entire remaining contents of the bag are flushed through a Whatman

355    Quartz microfibre filter (pre-fired at 550°C for 5.5 hours) to collect the particles. The filters were then wrapped in foil and stored at -18°C prior to analysis by LC-electrospray Orbitrap MS.

Actinometry and off-gassing experiments were conducted regularly through the programme in order to establish the consistency of the chamber's performance, evaluate the effectiveness of the cleaning procedure and confirm cleanliness of the chamber. Background filters were collected from the actinometry and off-gassing experiments.

360

## 4. Results

Photolysis of $NO_2$ under the simulated solar irradiation in the MAC forms $O_3$ and they rapidly move towards photostationary state with NO. The $O_3$ is photolysed at wavelengths below 310 nm to yield $O(^3P)$ and $O(^1D)$, the latter reacting with available water vapour to form the hydroxyl radical, OH. The $O_3$ will attack the double bond in unsaturated compounds such as $\alpha$-pinene

365    and isoprene, initiating oxidation and yielding secondary OH. The OH will attack all VOCs in the system, either by hydrogen abstraction or OH-addition. Owing to the isoreactivity concept employed in the experiments, the initial VOC destruction rate, and first-generation oxidation product production rate, at a *given* OH concentration will be the same, enabling the opportunity to explore interactions in the mixed systems. However, owing to the indirect method used to produce OH (and hence its production and loss rate and steady-state concentration) the loss rate of each VOC will be different, dependent on the

370    differential reactivity of the VOC towards $O_3$, and turnover of products from each will depend on this loss rate and the reactivity of their oxidation products to the prevailing oxidants. A currently unquantified contribution to the OH concentration will likely be contributed by the release from the walls of HONO, as has been seen in previous studies in Teflon reactors (Rohrer et al., 2005). This is under investigation and will influence the photochemical environment in the MAC, but does not directly change the results reported here.

375 To provide the photochemical context for example systems, Figure 1 shows time series of $NO_2$, NO and $O_3$ from experiments in the following 4 systems: α-pinene, isoprene, α-pinene/isoprene and o-cresol. Note that, in the presence of o-cresol, $O_3$ measurement by UV absorption was influenced by UV absorption by o-cresol and Figure 1(d) is corrected as explained in the methods section. Figure S1 shows the $NO_2$, NO and $O_3$ for all systems, similarly corrected for o-cresol containing systems.
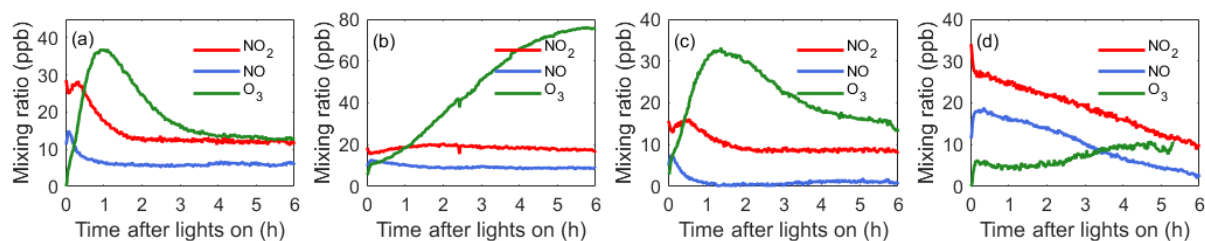


380 **Figure 1**: $NO_2$, NO and $O_3$ time series in example single and mixed VOC experiments (a) α-pinene, (b) isoprene, (c) α-pinene/isoprene, (d) o-cresol.

$O_3$ will move towards photo-stationary state (PSS) with NO and $NO_2$ according to reactions R1, R2 and R3:

$NO_2 + h\nu \rightarrow NO + O(^3P)$   (@ $\lambda < 424$ nm)   (R1)

385 $O(^3P) + O_2 (+ M) \rightarrow O_3 (+ M)$                    (R2)

$NO + O_3 \rightarrow NO_2 + O_2$                    (R3)
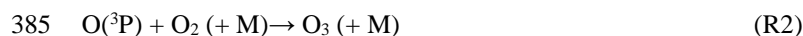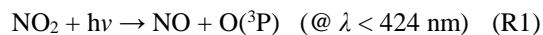
Some insight into the trajectory towards PSS across the systems can be gained by inspection of Supplementary Figure S2, which provides a comparative summary of the Leighton Ratio (Leighton 1961) for all systems and the $O_3$ calculated assuming PSS, i.e. Leighton Ratio of 1, shown for the o-cresol containing systems. The Leighton Ratio is given by

390 $\varphi = j_{NO2} [NO_2]/k_{O3+NO}[O_3][NO]$                    (1)

In the polluted high-NOx atmosphere, PSS universally applies and $\varphi$ is unity. In moderately polluted conditions, radical reactions are increasingly important in conversion of NO to $NO_2$ and typically $\varphi > 1$. This is because $HO_2$ and $RO_2$ will compete with the $O_3$ reaction for NO (R3) according to reactions (R4 and R5):

$HO_2 + NO \rightarrow NO_2 + OH$                    (R4)

395 $RO_2 + NO \rightarrow NO_2 + RO$                    (R5)

where RO$_2$ arise from biogenic VOC or *o*-cresol. Note that, in the ambient atmosphere, RO$_2$ can stem from a very wide pool of VOCs. Further deviation from PSS and consequent increase in $\varphi$ will occur when O$_3$ loss processes other than R3 become important. These can include reactions of O$_3$ with NO$_2$, alkenes and radicals. In our chamber systems, the O$_3$ reactions with $\alpha$-pinene and isoprene and radical reactions with NO, are competitive and provide substantial deviation from PSS. The NO$_x$ and

400   O$_3$ trajectories in the various systems can be seen to vary substantially. Nevertheless, in all systems, illumination of the chamber leads to the expected onset of significant photochemistry to initiate the VOC photo-oxidation.
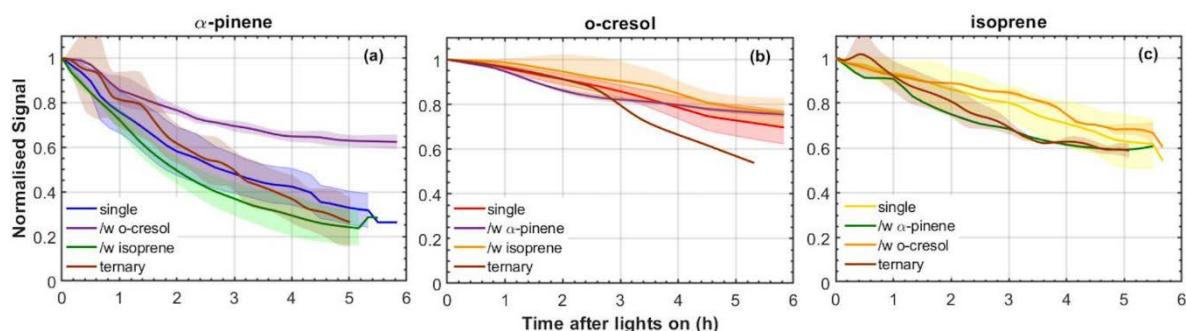


**Figure 2**: Decay rates of each VOC across all mixtures; a) $\alpha$-pinene, b) isoprene and c) *o*-cresol. All lines (and shaded areas)

405   containing blue correspond to experiments including $\alpha$-pinene, containing red to those including *o*-cresol and yellow to isoprene. For example, purple lines correspond to an α-pinene /*o*-cresol binary mixture and brown to the ternary mixture. The shaded areas represent 1 standard deviation around the solid line mean value of all experiments.

From Figure 2, it can be seen that the rate of decay is not the same in each experiment, despite the attempt at initial isoreactivity,

410   as explained in section 2.5. Oxidation products from each VOC will nevertheless be present in appreciable quantities in each experiment, satisfying the objectives of the design to enable exploration of interactions of oxidation products in SOA particle formation.

Figure 3 shows the time series of SOA particle mass in all experiments (with shading representing ± 1σ of the measurement across all experiments) in all precursor systems studied. It can be seen that the greatest SOA mass was generated in $\alpha$-pinene

415   containing systems, which is unsurprising, given the known efficiency with which it forms particle mass. It was found that *o*-cresol and *o*-cresol containing mixtures were the next most efficient at producing particle mass. This might be expected with its reported moderate SOA particle producing potential. Negligible SOA particles were formed in all single VOC isoprene experiments. Only when isoprene was in a mixture was any mass formed and, in all cases, this was lower than the mass formed

from the other VOC alone. Again, this is not too surprising, given the low or negligible particle mass yield reported for isoprene

420    on neutral particle seeds. As seen in Figure 2, not all VOC was consumed in all experiments and it can be seen that the particle

mass may not have fully peaked in all *o*-cresol and *o*-cresol / isoprene experiments. Nevertheless, the mass peak was observed

in most experiments before they were completed, and the chamber contents flushed through the filter for compositional

analysis. Panel b) in Figure 3 shows the SOA particle mass corrected for the losses of particles to the chamber walls. This was

conducted by calculating the exponential decay of particles of each size from a targeted ammonium sulphate wall loss

425    correction experiment performed close to the experiment of interest. Details of the wall loss correction can be found in Shao

et al. (2021a).
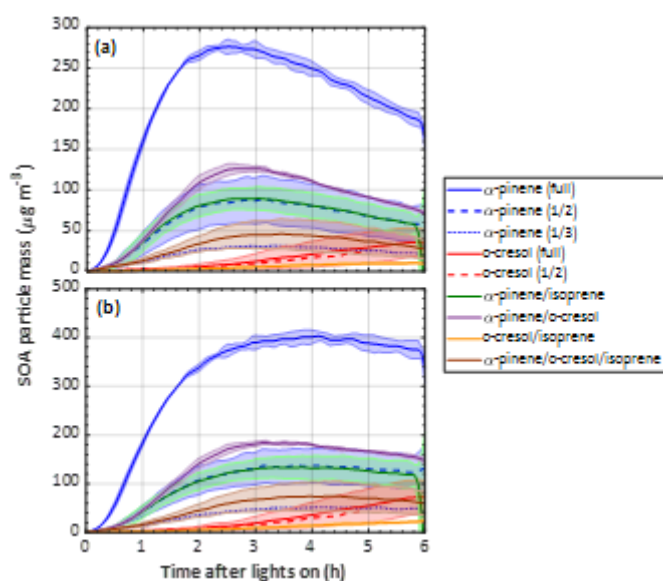


**Figure 3**: SOA particle mass (mean ± 1σ as shaded areas) in each system, a) raw measurements and b) particle wall-loss

430    corrected mass. Note that this is organic mass determined from AMS measurements and so does not include the ammonium

sulphate seed particles. The same colour scheme is used as in Figure 2.

Figure S3 shows the total particle wall loss corrected particle component mass ratios in each system indicating the inorganic

and organic component evolution as measured by AMS. As shown in panel a), the mass ratio of organic to inorganic seed

435    follows the production of SOA particle mass and the loss of total particle mass to the walls. In the wall loss correction, the

size-resolved loss of multi-component organic-inorganic aerosol particles is assumed to be the same as that for size-resolved

ammonium sulphate seeds loss rate measured in dedicated experiments (see methodology). The decrease in $SO_4^{2-}$/ $NO_3^-$ shown

in panel b) follows the wall loss of total particle mass (and hence $SO_4^{2-}$) and simultaneous oxidation of $NO_2$ by OH to form $HNO_3$ (and hence particulate $NO_3^-$). $NH_4^+$ was found to be in ion balance with the sum of $NO_3^-/SO_4^{2-}$ in all experiments.

440   Particle mass yield is a widely used metric that aims to represent the effectiveness of a VOC in forming SOA particle mass. In single precursor systems it is relatively straightforward the particle mass formed per unit of VOC consumed:

$$Y = \frac{\Delta[SOA]}{\Delta[VOC]} \qquad\qquad (2)$$

Frequently the yield is reported as a single number and this may be taken from measurements at maximum SOA particle mass formed in the experiment, at the maximum VOC consumed, or perhaps more arbitrarily, at the end of an experiment. Such

445   approaches may be reasonably applied for comparisons between precursors in identical oxidation conditions in the same chamber. Owing to significant particle losses to chamber walls, it can be seen from Figure 3 that it is important to correct the particle mass formed in the yield calculations for such losses. It is noted that the yields need to be corrected for VOC or OVOC product losses to the walls, too as discussed in section 5. Table 3 shows the calculated yields for all individual VOC and mixture experiments. The first 9 rows show the yields for single VOC experiments. Following the particle mass plots shown in Figure 3, it is clear that the efficiency in forming particle mass is in the order $\alpha$-pinene > $o$-cresol > isoprene, with no mass

450   yield observed in isoprene oxidation though appreciable isoprene consumption was observed as shown in Figure 2. For $\alpha$-pinene and $o$-cresol it can be seen that the yield increased with increasing initial concentration. The $o$-cresol and $o$-cresol / isoprene experiments were not continued to the point of maximum mass formation (as shown in Figure 3) and so the maximum VOC consumption and mass formation both correspond to the end of the experiments in these systems. Figure 4 shows the yield plotted against SOA particle mass for $\alpha$-pinene and $o$-cresol for all individual VOC experiments, indicating that the yield

455   increases monotonically with particle mass within propagated experimental uncertainties. Such behaviour is expected and is consistent with absorptive partitioning considerations. Note that organic mass formation in the "full reactivity" (i.e. 309 ppb $\alpha$-pinene) experiment is so rapid that VOC data are only available for yield calculation beyond 100 µg m$^{-3}$. Supplementary Figure S4 alternatively shows the SOA particle mass yield plotted against the total particle mass in the chamber, including the

460   ammonium sulphate seed particles that provide a condensation sink for the condensable vapours produced by VOC oxidation.
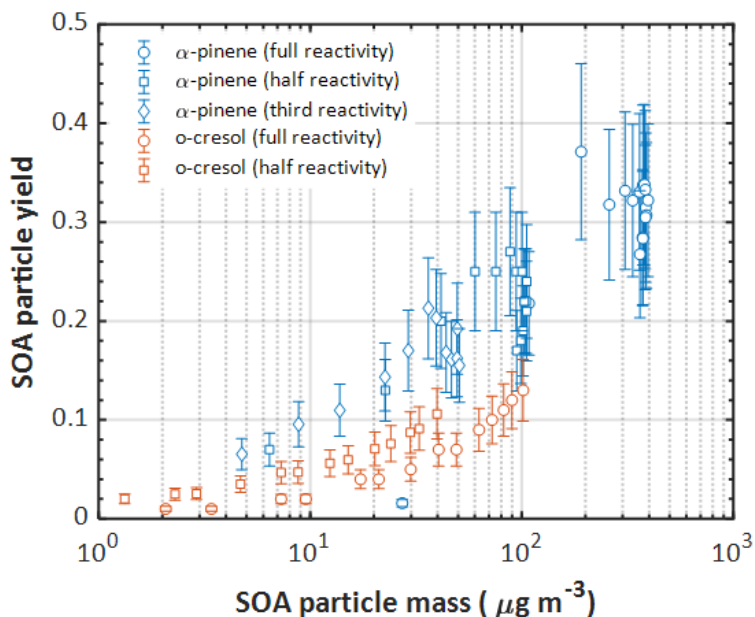
**Figure 4**: SOA particle mass yield as a function of mass formed in the single precursor α-pinene and *o*-cresol experiments at all initial concentrations. Error bars represent the propagated uncertainties in all measurements and in the particle wall loss corrections applied.

465    Since there is no SOA particle mass formed from isoprene, Table 3 additionally presents yield data omitting the consumption of isoprene in the denominator of equation 2, accordingly increasing the yield. Figure 5 shows the yield curves for typical experiments in all systems. The yield curves allow comparison between the systems, both including and excluding isoprene in the denominator of equation 2. The two-product model (Odum et al., 1996) was used to fit the yield curves for α-pinene and *o*-cresol. These are included to guide the eye. Here, the two-product model parameterised the relation of overall SOA yield

470    and the adsorptive mass assuming only two products to exist in the system. The equation of the two-product model is shown in eq.3. α, $K_p$ and $C_{OA}$ represent the stoichiometric factor, the partitioning coefficient of product and the total absorbing organic mass, respectively. The $\alpha_1$, $\alpha_2$, $K_{p,1}$, $K_{p,2}$ can be fitted from the yield curves.

475

**Table 3**: Measured and particle wall-loss corrected SOA particle mass yields for all systems calculated at maximum particle mass and maximum VOC consumed. For mixtures containing isoprene, which had zero yield on the neutral seeds injected, the yields were calculated excluding the consumption of isoprene in the system allowing them to be referenced to the mixtures without isoprene. Yield was calculated with the density of organic matter of $1.4 \mu g\ m^{-3}$. The maximum mass used in the yield at maximum mass calculation is given in Table 1. The uncertainties in SOA particle mass yield was calculated by propagating the $\pm 1\sigma$ uncertainties of measured $\triangle SOA$ and $\triangle VOC$.

| | Reactivity | Yield at max. mass | Yield at max. VOC consumed | Yield at max. mass (Isoprene excluded) | Yield at max. VOC consumed (Isoprene excluded) |
|---|---|---|---|---|---|
| α-pinene | Full | $0.32 \pm 0.08$ | $0.27 \pm 0.06$ | | |
| | 1/2 | $0.21 \pm 0.05$ | $0.17 \pm 0.04$ | | |
| | 1/3 | $0.16 \pm 0.04$ | $0.13 \pm 0.03$ | | |
| isoprene | Full | 0 | 0 | | |
| | 1/2 | - | - | | |
| | 1/3 | 0 | 0 | | |
| o-cresol | Full | $0.13 \pm 0.03$ | $0.13 \pm 0.03$ | | |
| | 1/2 | $0.11 \pm 0.03$ | $0.11 \pm 0.03$ | | |
| | 1/3 | - | - | | |
| α-pinene/isoprene | Full | $0.16 \pm 0.05$ | $0.13 \pm 0.04$ | $0.19 \pm 0.05$ | $0.16 \pm 0.04$ |
| α-pinene/o-cresol | Full | $0.29 \pm 0.09$ | $0.22 \pm 0.07$ | | |
| o-cresol/isoprene | Full | $0.06 \pm 0.02$ | $0.06 \pm 0.02$ | $0.08 \pm 0.02$ | $0.07 \pm 0.02$ |
| α-pinene/o-cresol/isoprene | Full | $0.11 \pm 0.04$ | $0.08 \pm 0.03$ | $0.12 \pm 0.04$ | $0.08 \pm 0.03$ |

In addition to the measured points, Figure 5 shows "predicted" yields for the mixtures, based on the organic mass at the same VOC consumption measured in the single VOC experiments and additively combining them according to:

$$Yield = C_{OA}\left(\frac{\alpha_1 K_{p,1}}{1+K_{p,1}C_{OA}} + \frac{\alpha_2 K_{p,2}}{1+K_{p,2}C_{OA}}\right) \quad\quad (3)$$

and

$$Yield_{pred.} = \frac{\Delta m_{\Delta VOC1} + \Delta m_{\Delta VOC2} + \Delta m_{\Delta VOC3}}{\Delta_{VOC1} + \Delta_{VOC2} + \Delta_{VOC3}} \quad\quad (4)$$

490    The parameters for the two-product fit from the single VOC half- and third-reactivity experiments were used to generate a yield-mass-ΔVOC look-up-table. This was then used to calculate the particle mass formed from each precursor at the consumption of the VOC at each point in the binary and ternary systems.
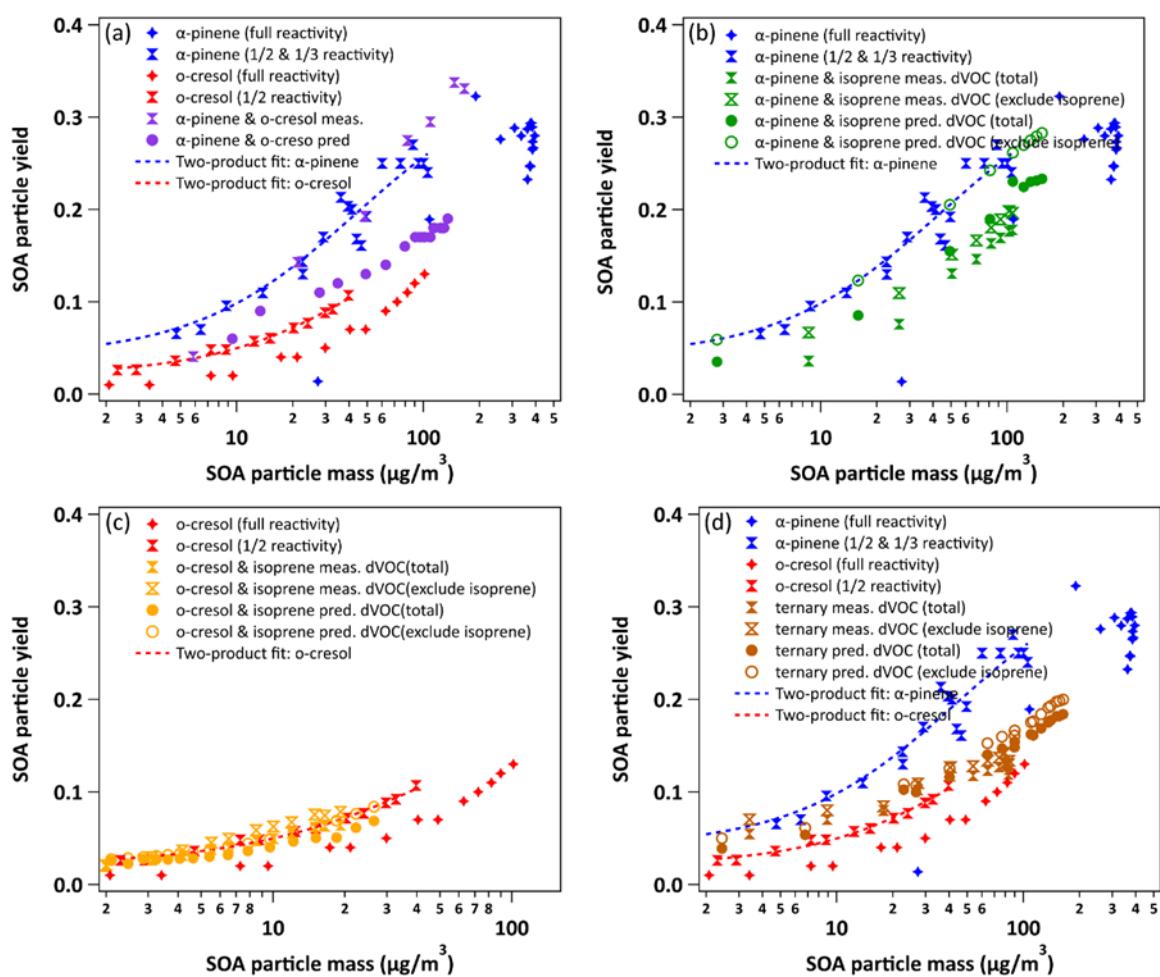


**Figure 5**: Yield data for selected representative experiments in all systems (with 2-product yield curves for α-pinene and *o*-cresol single VOC experiments). Panel a) shows the binary α-pinene / *o*-cresol mixture and its constituents, b) the binary α-pinene / isoprene mixture, c) the *o*-cresol / isoprene mixture (expanded y-axis plot shown in Figure S5) and d) the ternary α-

pinene / $o$-cresol / isoprene mixture. Yields "predicted" from the linear combination of yields from the individual VOC
500    experiments using equation 4 are shown for each mixture.

Using this look-up table, the predicted yield from the binary α-pinene / $o$-cresol mixture photo-oxidation is below that measured
in the α-pinene / $o$-cresol mixture experiment and slightly higher than that in the individual $o$-cresol experiment at 50%
reactivity. Indeed, the yield measured in the mixture is comparable to that of α-pinene at one half and one third reference
505    reactivity. For the isoprene-containing binary mixtures, clearly the predicted yield excluding isoprene in the denominator is
identical to that of the 2-product curve fitted to the single VOC experiment derived yield of other components in the mixtures.
In the α-pinene / isoprene system, the predicted yield accounting for the consumption of both α-pinene and isoprene is higher
than that measured but, as shown in Tables 3 and 4, comparable to the measured yield referenced only to the consumption of
α-pinene. In the $o$-cresol / isoprene system, the predicted yield accounting for the consumption of both $o$-cresol and isoprene
510    is lower than that measured (at higher mass loadings), there is little difference within uncertainty at a lower mass. The predicted
yield accounting for the consumption of $o$-cresol alone is lower than that measured when referenced to the same total VOC
consumption, but comparable to the measured yield referenced to the consumption of both $o$-cresol and isoprene. Finally, in
the ternary system, the predicted yield excluding isoprene consumption is similarly (and obviously) higher than that including
its consumption, but both predictions are between the yields of single α-pinene and $o$-cresol experiment measurements. The
515    measured yields accounting for only α-pinene and $o$-cresol consumption in the ternary mixture are also similarly (and
obviously) higher than that including isoprene consumption. There is insufficient difference between the measurements or the
predictions to state whether inclusion or exclusion of isoprene consumption gives a much better agreement, though there is an
indication that the predicted yields show a steeper gradient with SOA particle mass than the measured slope, which more
closely follows that of the $o$-cresol than that of α-pinene. Table 4 distils the predictions based on the yield from single VOC
520    experimental data at the same consumption as in the mixtures into single values predicted at maximum SOA particle mass,
maximum VOC consumption, both with and without isoprene decay in the calculation.

To explore the likely fate of the parent VOCs in the MAC, we used the measured $O_3$ concentrations and VOC decay rates and
exploited the differential reactivities of the VOCs to investigate the decay attributable to each oxidant and also overcome
measurement difficulties encountered in the experiments. For example, knowing that $o$-cresol has a negligible rate of reaction
525    with $O_3$, we are able to calculate the OH concentration from the $o$-cresol decay curve. This can then be used to attribute the
fraction of the decay of isoprene and α-pinene to OH and $O_3$ in their binary mixtures with $o$-cresol. This is important, since the
measurement of $O_3$ by UV absorption in the presence of $o$-cresol is challenging and requires correction for the additional
absorption by $o$-cresol. In systems without $o$-cresol, the decremental decay attributable to $O_3$ can be constructed for α-pinene
and isoprene using the $O_3$ measurements and (reaction rates of 9.6 and 1.28 x $10^{-17}$ cm$^3$molecules$^{-1}$ s$^{-1}$, respectively; Cox et al.,

530    2020), by comparing with the actual $\alpha$-pinene and isoprene, the residual decay can be attributed to OH. An example of this oxidant reconciliation is shown in Figure 6 for the binary $\alpha$-pinene / isoprene system.

**Table 4** SOA predicted yield for the 4 mixtures at maximum SOA particle mass produced and maximum VOC consumed. The uncertainties in SOA particle mass yield was calculated by propagating the $\pm$ 1$\sigma$ uncertainties of predicted $\triangle$SOA and 535    measured $\triangle$VOC.

| | **Predicted Yield at:** | | | |
|---|---|---|---|---|
| | **Max. SOA particle mass** | **Max. VOC consumption** | **Max. SOA particle mass excl. isoprene** | **Max. VOC consumption excl. isoprene** |
| $\alpha$-pinene/isoprene | 0.19± 0.08 | 0.15±0.06 | 0.21±0.08 | 0.17±0.06 |
| $\alpha$-pinene/$o$-cresol | 0.17±0.07 | 0.14±0.05 | 0.17±0.07 | 0.14±0.05 |
| isoprene/$o$-cresol | 0.10±0.04 | 0.09±0.04 | 0.11±0.04 | 0.11±0.04 |
| $\alpha$-pinene/isoprene/$o$-cresol | 0.13±0.06 | 0.11±0.05 | 0.14±0.05 | 0.12±0.05 |
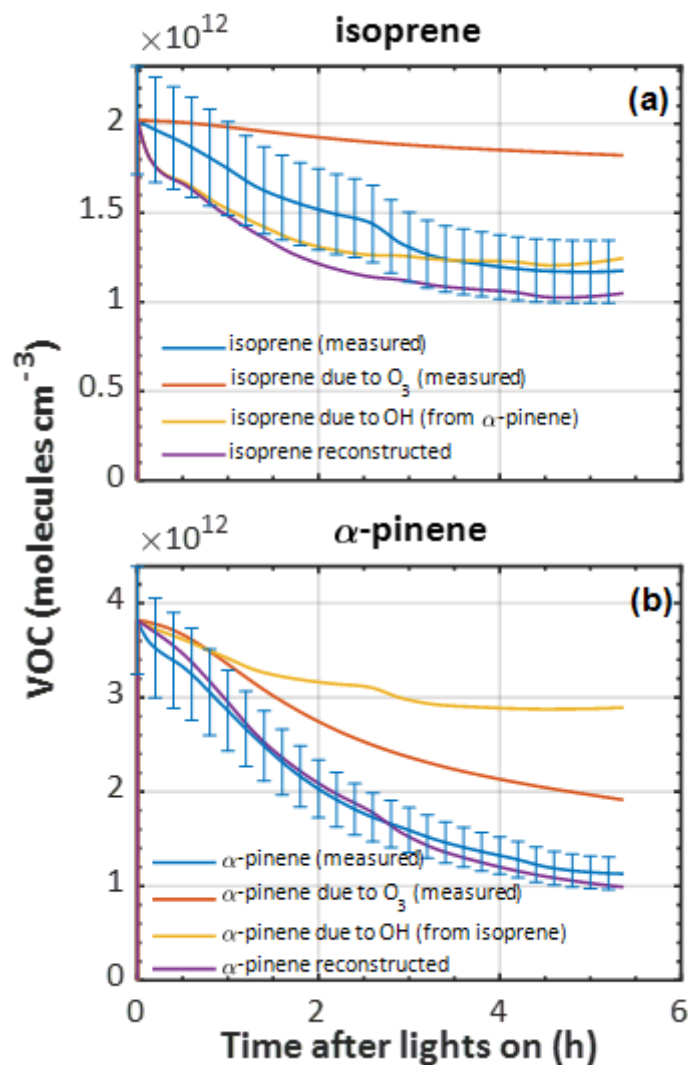
**Figure 6**: Measured ( ±15% error) and reconstructed (a) isoprene and (b) α-pinene  decay in a α-pinene & isoprene binary
experiment. Initially, in each case the decay of the VOC due to ozone was predicted based on the $O_3$ concentration, the reaction
rate of each VOC toward $O_3$ and the initial VOC concentration. Subsequently, the OH concentration from each VOC was
estimated from the difference in the VOC decay attributed to $O_3$, and the measured VOC decay. Finally, the OH concentration
from each precursor was used to reconstruct the decay of the other (i.e. OH from isoprene was used to reconstruct the decay
of α-pinene and vice versa.

In the example shown in Figure 6, it can be seen that roughly twice as much loss of $\alpha$-pinene can be attributed to $O_3$ as to OH and roughly 4 times as much isoprene loss attributed to OH as to $O_3$. The inability to control isoreactivity towards all oxidants through controlling the initial VOC concentrations will influence prediction of SOA particle mass yields owing to the differences in tendency to condense of oxidation products from different oxidants. These aspects are discussed in section 5.

550    Differences in the SOA particle oxgenation trajectory between the systems are illustrated in Figure 7 by the percentages of the AMS total signal at m/z=44 ($f_{44}$) and 43 ($f_{43}$) respectively to represent more and less oxygenated contribution to the SOA particle mass.
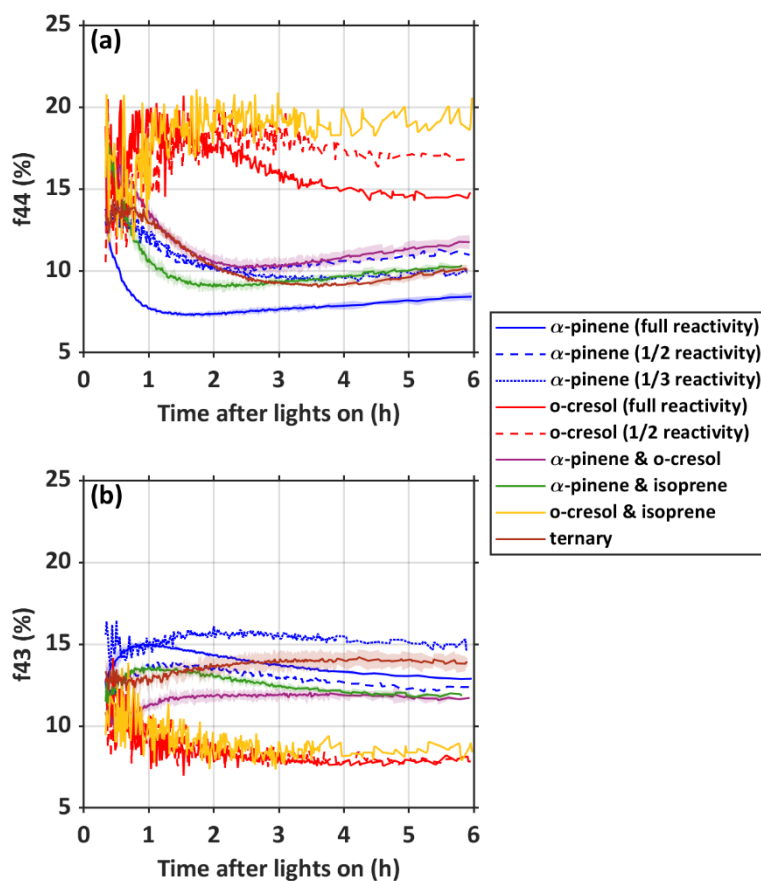


**Figure 7**: Aerosol Mass Spectrometer time series of $f_{44}$ and $f_{43}$ in all systems.

555

25

With some simplification $m/z=44$ is the $CO_2^+$ fragment thought to be formed by decarboxylation on the AMS vapouriser and $m/z=43$ corresponds to the presence of less oxidised components like carbonyls (though with a small contribution from unoxidised alkyl fragment ions that was not substracted). The full reactivity single VOC $\alpha$-pinene experiment has the lowest $f_{44}$ and highest $f_{43}$ of all systems. Systems that do not contain $\alpha$-pinene can be seen to comprise a persistently higher $f_{44}$ and

560  lower $f_{43}$ than all $\alpha$-pinene containing systems. This is attributable to a higher contribution of the mass from products of $\alpha$-pinene with a lower degree of oxygenation, when it is present in the mixture. However, there is a substantial difference in the fractional contributions of the fragments with concentration in the single VOC $\alpha$-pinene experiments, with higher $f_{44}$ in the lower concentration experiments forming lower mass. This may be partly explained in terms of absorptive partitioning, with lower absorptive mass enabling condensation of only the lower volatility (and more oxidised and higher $f_{44}$ products). However,

565  such effects would likely be small since the mass reduction is not large. Moreover, the difference between $f_{44}$ at full and half reactivity might be expected to be smaller than that between half and third reactivity since the mass difference is smaller between the former pair of experiments. However, the reverse is true. The high $f_{44}$ generated in the $o$-cresol systems and persisting through to high masses later in the experiments is notable and suggests that a high degree of oxygenation is required to enable partitioning of these compounds to the particles (Emanuelsson et al., 2013) . Compared with the lower degree of

570  oxygenation required in the $\alpha$-pinene systems, it may indicate the requirement for molecules derived from the smaller $C_7$ precursor to be more oxygenated than those from its $C_{10}$ counterpart. The attribution of the m/z=44 fragment to di- and polycarboxylic acids is interesting in this context, given the high fractional signal contribution of $C_7H_7NO_4$ isomers from CIMS and UPLC-Orbitrap MS, see text below and Figure 10. This chemical behaviour has been re-expressed in Figure S6 following the approach first described in Ng et al. (2010). It can be seen that the systems all fall to the right of the delineated triangular

575  area bracketing ambient atmospheric behaviour – a finding frequently observed in many chamber systems (see e.g. Figure 4 in Alfarra et al., 2013). A more thorough analysis of the composition from analysis of the high resolution AMS data is the subject of a separate manuscript (Shao et al., 2021a, in prep.).

A further illustration of the differences in the chemical trajectories can be provided by the time series of gaseous and particulate components derived from the FIGAERO-I$^-$-CIMS instrument. Figure 8 illustrates the changes in particulate mass spectra of

580  single $\alpha$-pinene and $o$-cresol experiments and their mixture. These mass spectra have been normalised to the same reagent ion concentration. There is a clear increasing signal in the m/z range from 200 to 600 (I- adducts) after 5.5-hour reactions in single and mixture systems corresponding to the increase in detected particulate products with the increase in SOA particle mass with time. Additionally, some unique peaks (e.g., m/z 358, 403, 419, 439, etc) are only detected in the mixture mass spectra. Peak assignment of these mass spectra has been used to attribute signal to the molecular formulae and hence to broad chemical

585  groupings in all single VOC and mixed systems. A full analysis and discussion can be found in Du et al., 2021 (in prep).
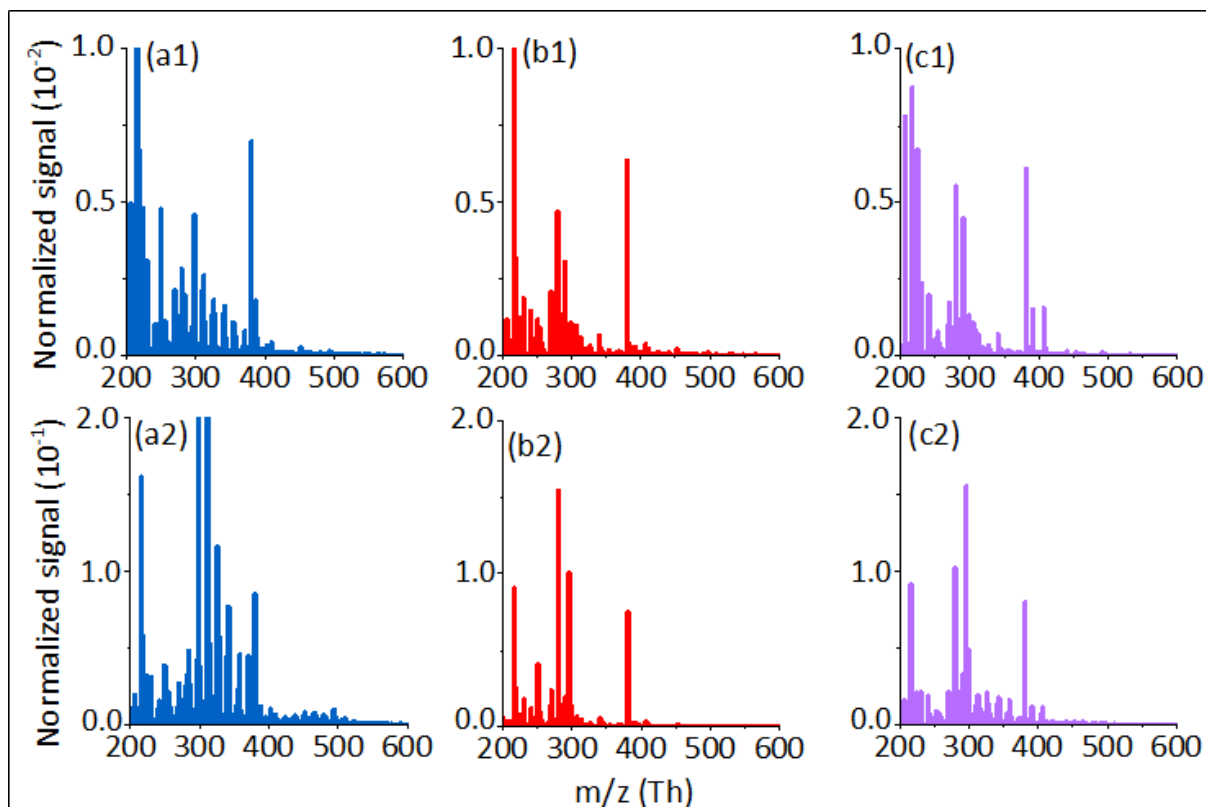
**Figure 8**: FIGAERO-CIMS Mass spectra taken in the single precursor $\alpha$-pinene (a1 and a2), o-cresol (b1 and b2) and mixed $\alpha$-pinene / o-cresol system (c1 and c2) at 0.5 hour (a1, b1 and c1) and 5.5 hours (a2,b2 and c2) after the onset of photochemistry in the MAC.

590

Owing to its separation and accurate mass resolution, the LC-Orbitrap MS analysis of extracts of particles from the filters collected at the end of the experiments provide molecular information to gain insight into interactions in the mixed systems. Figure 9 illustrates the ability to attribute signal in the filter extracts of particles in the ternary *o*-cresol / $\alpha$-pinene / isoprene mixture to the individual parent VOC (by matching the attributed formulae to those identified in the individual precursor

595 experiments) and thereby identify molecules found only in the mixture with their associated fractional signal contribution. This is shown for molecules detected in negative, panel a), and positive ionisation mode, c). These "unique-to-mixture" components have been split by contribution to the signal by carbon number in panels b) and d) for negative ion and positive ion mode respectively. These analyses are presented and expanded upon for all mixtures in Shao et al., 2021b (in prep.). Clearly a substantial fraction of the unique-to-mixture signal is found at carbon number greater than any precursor VOC (in -ve

600 ionisation mode 57% of the signal in 48 individual peaks with nC > 10 and in +ve mode 60% in 115). Whether such components

27

result from gaseous or condensed phase reactions is not accessible from these measurements, but they clearly result from interactions in the mixture.
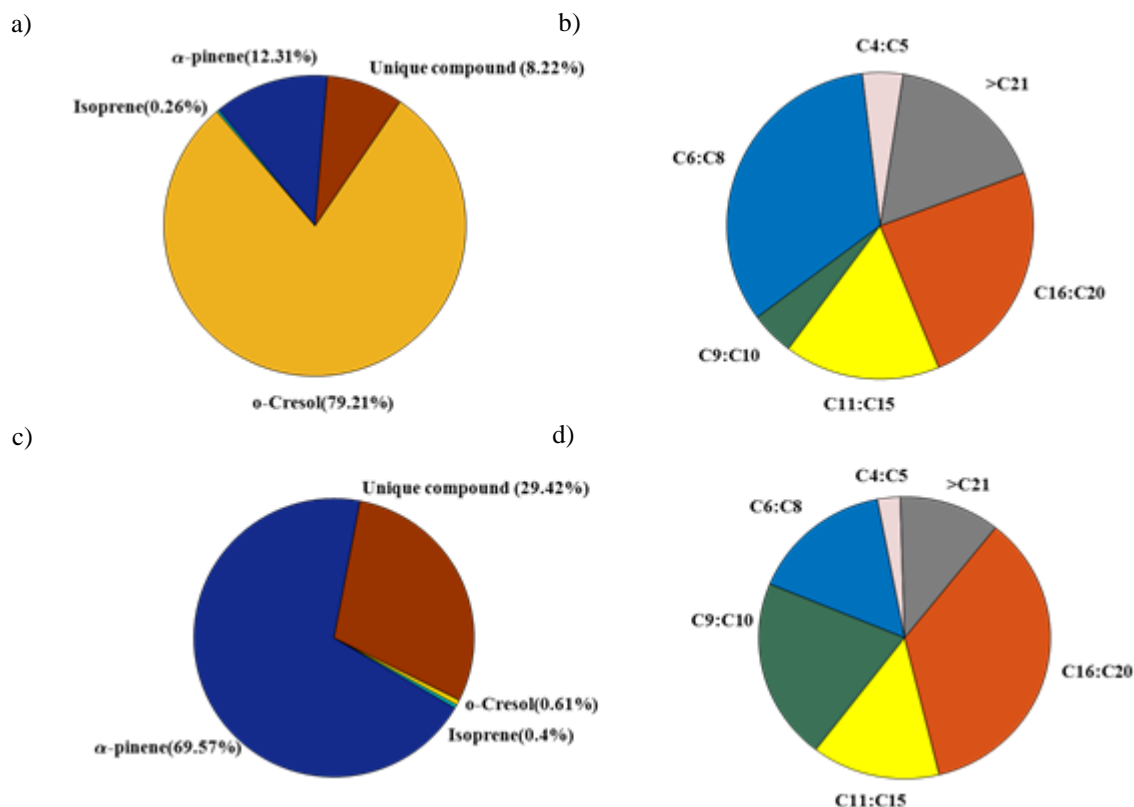


**Figure 9**: Molecular resolved compounds in the particle phase for the ternary $o$-cresol / $\alpha$-pinene / isoprene mixture obtained using UPLC-Obitrap MS of filter extracts: a) fraction of signal in negative mode, b) fraction of signal by carbon number in the unique-to-mixture compounds, c) fraction of signal in positive mode, d) fraction of signal by carbon number in the unique-to-mixture compounds

Panel a) in Figure 10 expands on the molecular attribution by LC-Orbitrap MS to demonstrate the ability to separate isomeric contributions to the signal normalised to the total detected signal in single precursor and mixed systems. The example shown is for $C_7H_7NO_4$ (methyl-nitrocatechol and its isomers) in $o$-cresol containing systems. It can be seen that the isomer at an LC retention time of 9 minutes dominates the signal in all systems, whilst the isomer at retention time of 6.1 minutes displays negligible signal fractions in all systems. In contrast, the I$^-$-CIMS is incapable of separating structural isomers. Panel b) shows

the time series of the total signal at m/z=296 (normalised to the total attributed signal) corresponding to the combined signal

615    from all $C_7H_7NO_4$ isomers in the same systems.
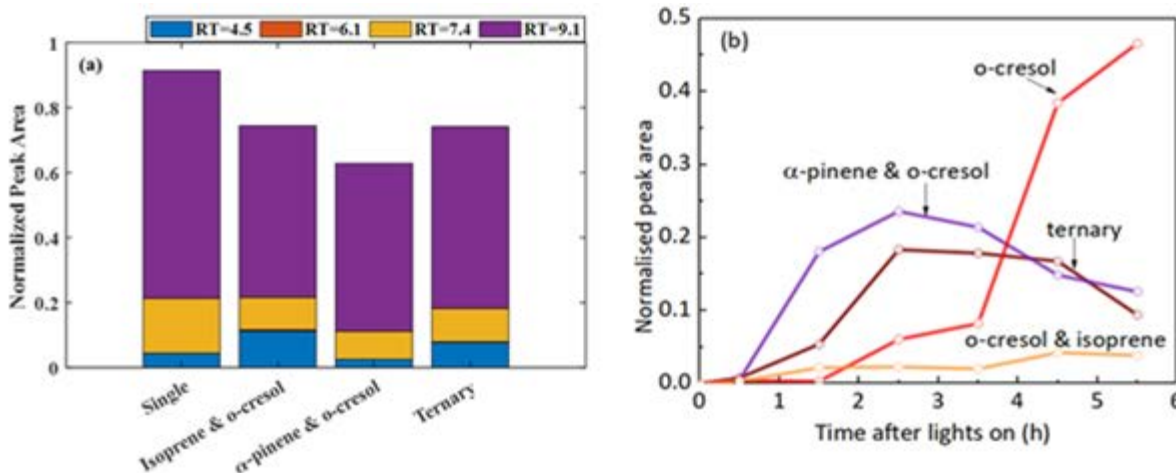


**Figure 10**: a) changes in the isomeric fractions of $C_7H_7NO_4$ across *o*-cresol containing systems from LC-Orbitrap MS analysis of the filter extracts collected at the end of each experiment; b) time series of particulate $C_7H_7NO_4$ from FIGAERO-CIMS

620    The attribution of elemental composition in the high resolution FIGAERO-CIMS analysis enables a comprehensive mapping of the particulate oxygen to carbon ratio (O:C) as a function of carbon number, as shown in Figure 11 for each system. It can be seen that the majority of signal in the *o*-cresol single system comprises compounds at the same carbon number, $C_7$, as the parent and, on average, with slightly higher O:C ratios than $C_{10}$, products dominating the *α*-pinene single VOC system. A significant fraction of the signal in all *α*-pinene containing systems is found at carbon numbers corresponding to the "dimer"

625    range and these are all found predominantly in the particle phase (showing a low volatility). Interestingly, these low volatility products are absent in the mixtures containing *α*-pinene and *o*-cresol, suggesting a potential increase of the overall volatility. At the same time, a range of new products appear in mixtures (e.g. *α*-pinene / *o*-cresol, *o*-cresol / isoprene) with higher carbon numbers (nC=11-16), lower O:C (O:C<0.5) and varying volatility ($\log_{10}C^*$=1-3 ), indicating that the molecular interactions influences the overall SOA particle volatility. A more complete discussion of the chemical composition variation across the

630    mixtures in the gas and particle phases can be found in Du et al. (2021, in prep.) and Voliotis et al. (2021b, in prep.).
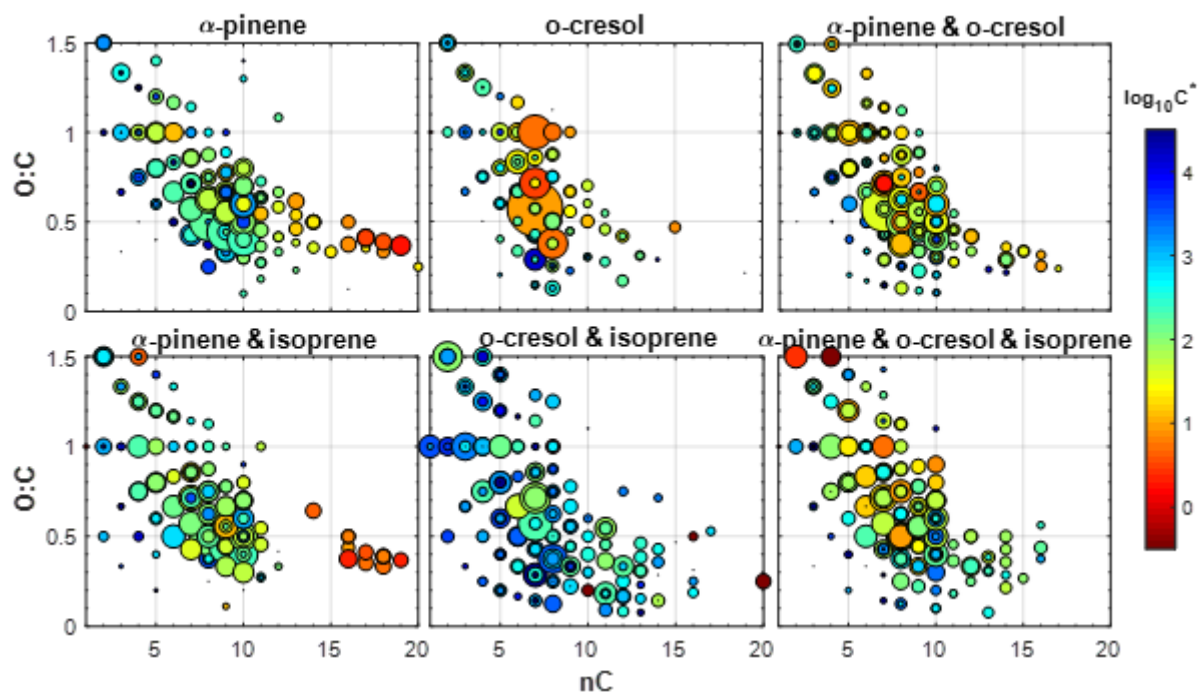
**Figure 11**: Oxygen to carbon ratio (O:C) vs carbon number (nC) of all the products identified by the FIGAERO-I⁻-CIMS in the particle phase at the end of each experiment in characteristic experiments in each system. Dots are sized based on the square root of the contribution of each product to the total signal and coloured according to their effective saturation concentration (C*). The C* was calculated using the gas to particle ratio of each ion and absorptive partitioning calculations.

The calculation of the C* of all identified formulae by performing partitioning calculations using the gas to particle ratio of the ions (Voliotis et al., 2021a) can be used to assemble the volatility distribution of the products, as shown for the single VOCs, their binary and ternary mixtures in Figure 12. It can be seen that the volatility distributions of particles in the mixture experiments can be similar (α-pinene / isoprene) or quite different (o-cresol/isoprene) to those in the experiments using the single precursor. These observations suggest that the effect of mixing precursors can have a varying effect on the resultant particle volatility. A full discussion of the chemical composition and its influence on volatility in all systems can be found in Voliotis et al. (2021b, in prep.)
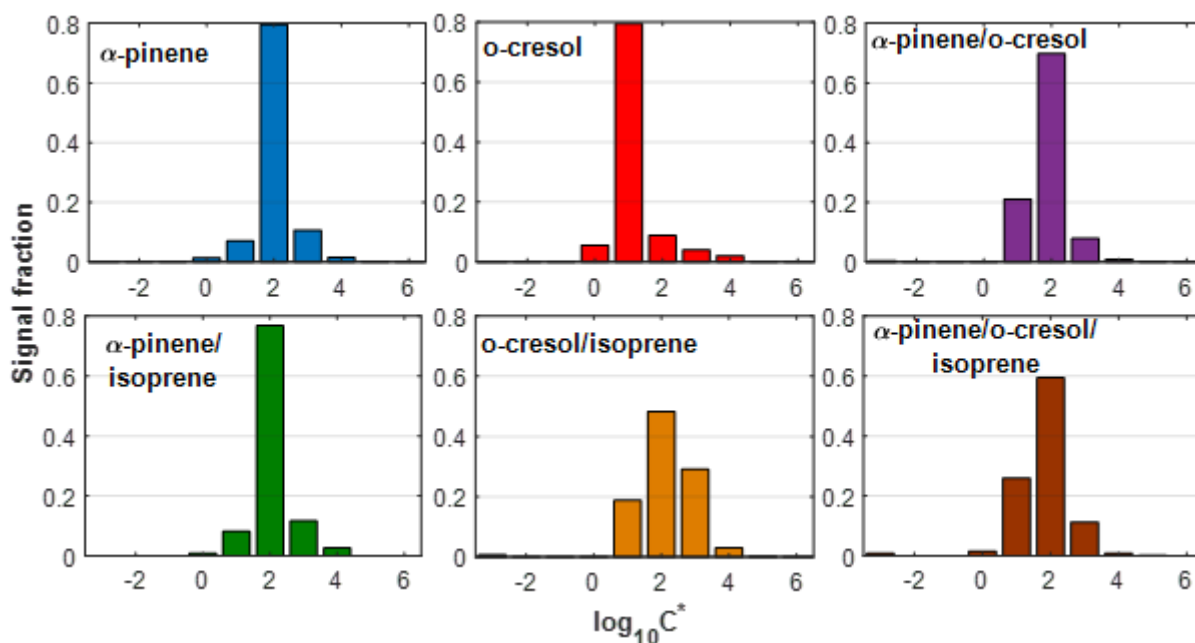
**Figure 12**: Volatility distributions expressed as effective saturation concentration (C*) in the volatility basis set framework of
645 all the products identified by the FIGAERO-CIMS as a function of the total particle phase signal in example experiments in
all systems. The C* was calculated using the gas to particle ratio of each ion and absorptive partitioning calculations.

The differences in evolution of the SOA particle components and the total mass formed directly influences the particle
properties as expected. Since the particles are grown on inorganic seeds, the physical properties in all systems are initially
650 dominated by the inorganic components as shown in Figure 13. This shows the relationship between the multicomponent
particle composition, the hygroscopic growth factor and the rebound fraction of particles (indicative of their phase state) as the
SOA to inorganic mass fraction of the particles develops in 3 example systems (*o*-cresol / isoprene, *o*-cresol and *α*-pinene).
The hygroscopicity much more rapidly decreases in systems where organic material is more rapidly formed and the transition
to a higher fraction of particles rebounding on a filter at high RH is similarly more rapid. It is clear that the rate of change of
655 organic to inorganic ratio plays a controlling role in physical behaviour of the particles. The evolution of both these properties
across all systems is discussed in detail in Wang et al. (2021a, b).
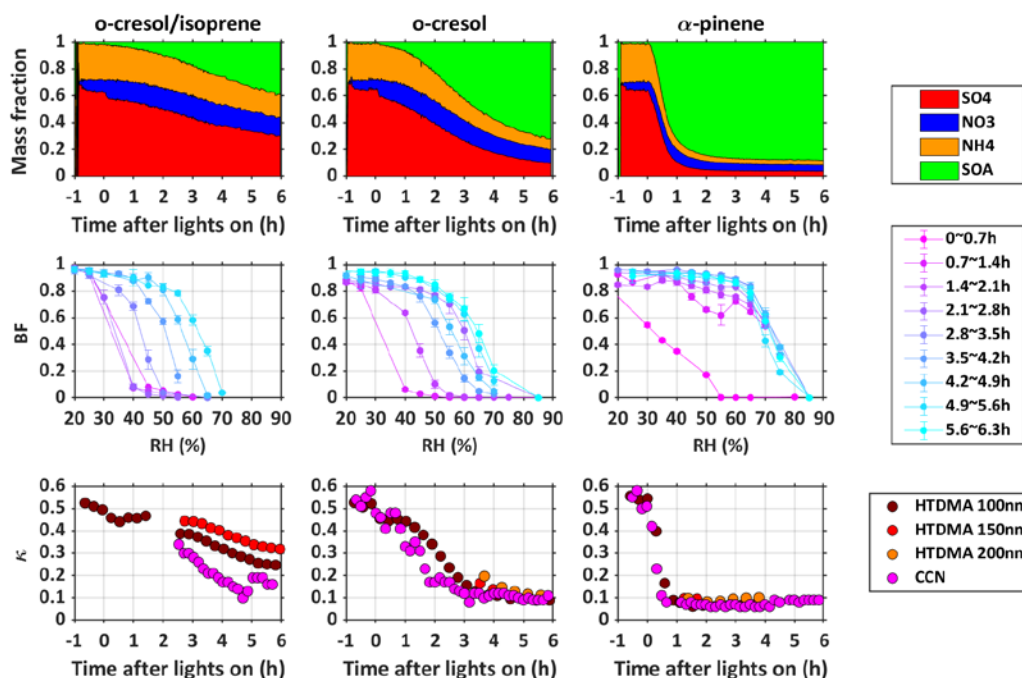
**Figure 13**: top row: AMS chemical composition showing rate of production of SOA and hence rate of increase in organic to
inorganic ratio moving from left to right (from *o*-cresol / isoprene to *o*-cresol to *α*-pinene); middle row: the corresponding
increasingly rapid transition to increased Bounce Fraction (BF) at higher RH; bottom row: the corresponding increasingly
rapid reduction in the hygroscopicity parameter, k.

## 5. Discussion

### 5.1. Experimental conditions and photochemistry

The control of photochemical conditions in VOC mixtures is challenging. The chemical space is multidimensional and non-
linear, and it is unclear how best to define the regime for direct comparison across systems. The approach taken in the current
study, to start with concentrations of each VOC isoreactive towards a single oxidant cannot account for the differential
reactivity towards the two oxidants, $O_3$ and OH, present in the system. This is particularly true when the production of oxidants
is tightly coupled to the VOC oxidation itself and secondary oxidant production can be at a comparable level to primary
production. The combination of oxidants can lead to significantly different VOC decay and hence turnover of oxidants and

products. This is an unavoidable feature of VOC mixtures that will occur in the real atmosphere and such differences need to be carefully considered in the interpretation of the results.

It can be seen from Figures 1 and S1 that the time profiles of NOx and $O_3$ vary substantially across the single precursor
675　experiments and the mixtures. This is a characteristic of the method of initiating photochemistry in our experiments, through photolysis of a VOC / NOx mixture in the initial absence of $O_3$. Within the same single VOC systems, the $O_3$ concentration temporal profile can vary with VOC concentration at the similar VOC/NOx values. It is particularly notable in the $\alpha$-pinene experiments owing to its reactivity towards $O_3$. As expected, there is a more ozone production in some systems (notably those containing isoprene). The Leighton ratios shown in Figure S2 indicate wide variation in the deviation from PSS across the
680　systems, with the high concentration single VOC $o$-cresol experiments and the $\alpha$-pinene / $o$-cresol and $\alpha$-pinene / isoprene binary mixtures showing the greatest +ve deviation (i.e. greatest ability for $RO_2$ and $HO_2$ to compete with $O_3$ for NO), whereas the single VOC isoprene and $\alpha$-pinene, binary isoprene / $o$-cresol and ternary systems all move towards low $\varphi$ -values.

It was shown in Figure 2 that the turnover of each VOC was different, likely resulting from the differential reactivity of each VOC towards the different oxidants present in the systems at any one time. However, it can be seen that the turnover of each
685　individual VOC was comparable across each system (with the notable exceptions of decreased $\alpha$-pinene turnover in its binary mixture with $o$-cresol and slightly increased $o$-cresol turnover in the ternary mixture). This may be i) coincidental, ii) indicative that the oxidant regimes remain comparable between experiments or iii) indicative that the turnover is relatively insensitive to the change in oxidant regimes between the mixtures in our experiments. Figure 1 and S1 show the differences in $O_3$ across systems, so the differences in oxidants are likely to be non-negligible (option ii)). In relation to the turnover with respect to
690　each oxidant in a mixed oxidant system, it should be borne in mind when comparing the results from different studies that results may diverge if the dominant oxidant changes. For example, Figure 6 shows that in the MAC $\alpha$-pinene / isoprene experiments, roughly twice as much $\alpha$-pinene consumption was due to $O_3$ reaction as to OH consumption. By contrast, in the experiments in the Julich Plant Aerosol Chamber reported in McFiggans et al. (2019) around 90% of the consumption was estimated to result from OH reaction.

695　Control of the oxidant regime in chamber experiments is strongly dictated by the goals of the study. It is perhaps most straightforward in a dark system in the absence of NOx, where only $O_3$ is being introduced with a single unsaturated VOC. Even then, the chemical regime can change as the oxidant is consumed and moves from excess to limited. Moreover, the yield of OH from ozonolysis can be non-negligible, such that the VOC consumption from the OH oxidation must be considered. A dark OH source (such as ozonolysis of TME) can be used for oxidation of a saturated VOC to access the OH decay relatively
700　"cleanly", though the possibility for interaction between the source VOC and SOA precursor derived $RO_2$ must be remembered. Dark oxidation by continuously injected $NO_3$ in the absence of $O_3$ can also provide a "clean" system with relatively few interfering pathways. $NO_3$ generated from $O_3$ reaction with $NO_2$ starts to become quite complex. The competition between oxidants in establishing the dark consumption of unsaturated VOC will be challenging, though the $NO_3$ reaction can dominate

in systems containing phenolic compounds such as *o*-cresol. In illuminated systems, the oxidant regime becomes complex

705　quite quickly. Photo-oxidation in the absence of NOx can access OH consumption of saturated compounds more straightforwardly than for unsaturated VOCs, where ozonolysis (and its associated secondary OH source) must be considered. Photo-oxidation in the presence of NOx introduces about as much complexity as can be envisaged. Photo-oxidation of multiple VOCs in the presence of NOx multiplies this complexity. The study of McFiggans et al. (2019) avoided many of the challenges faced in the current study by considering the mixture of biogenic VOCs in the absence of NOx and in a regime dominated by

710　OH oxidation. This can be considered reasonable, since mixtures of these VOCs might exist in the clean troposphere, remote from anthropogenic sources. In studying mixtures of anthropogenic and biogenic VOCs, it might be considered less reasonable since anthropogenic VOCs would seldom exist in the absence of appreciable NOx. Related to this, it should also be noted that, whilst maintaining the VOC : NO$_x$ ratio relatively constant across the systems is desirable, with reduced VOC concentrations this will lead to reduced NO concentrations. This will inevitably lead to reduced OH concentrations and hence VOC turnover.

715　This is of importance when comparing the single VOC experiments at different concentrations, but less important when considering the initially isoreactive mixtures, since the VOCs have been chosen for their reactivity such that their concentrations are at least of comparable magnitude at comparable mixture reactivity.

One feature of chamber experiments using mixtures of VOCs is the ability to exploit their differential reactivity towards the oxidants present in the system to attribute their decay to each of them. This reconciliation of the VOC decay, as shown in

720　Figure 6, is potentially a powerful interpretive tool for diagnosis of the concentration of oxidants in the system and understanding of the turnover of VOCs in the system practice. In our systems when *o*-cresol is present, there are limitations owing to the interference of the direct O$_3$ measurements owing to absorption of UV by *o*-cresol. However, the reconciliation in these cases can be used to aid validation of the correction based on CIMS measurement of *o*-cresol (see methods section 3). It should be noted any absorption by *o*-cresol oxidation products can still lead to bias in the reconciliation since O$_3$ will be

725　underestimated. Clearly, direct measurement of OH could provide additional confidence in the oxidant field but adequate constraint can be provided by the indirect method described here.

A final consideration relates to the exploratory nature of the current study which aims to establish the suitability of the approach to reveal aspects of SOA formation in mixed VOC atmospheric systems inaccessible to experiments using a single precursor species. The broad suite of analytical techniques employed to investigate these aspects have varying requirements and some

730　compromises have been necessary. Most importantly, the offline filter analyses require a minimum particle mass loading with the corresponding consumption of VOCs with varying yield. This has necessitated the use of initial VOC concentrations above ambient levels. Whilst such concentrations have been commonplace in chamber experiments, they do introduce limitations. Figure S2 indicates that the deviation from PSS is likely to be significantly affected by the reactions of RO$_2$ (and / or HO$_2$) with NO in some of the binary mixtures. One further important limitation arises from the non-scalability involved with

735　processes that are higher than first order. Peroxy radical terminations often involves their cross-reaction which will be in

competition with other bimolecular pathways; so, reactions that are second order in peroxy radical concentration will be in competition with those that are first order. This will be important in the termination of peroxy radicals formed during autoxidation leading to HOM formation. In particular, the reactions of large HOM-RO$_2$ with other large peroxy radicals leading to gas phase formation of accretion products in the "dimer" range may be over-represented at higher concentrations. Under

740 clean ambient conditions, their reaction partners would likely be dominated by HO$_2$ from CO oxidation, or smaller organic peroxy radicals such as CH$_3$O$_2$ from CH$_4$ oxidation. Under more polluted conditions, the alkoxy pathways from NO reaction will be competitive or even dominant. Each of these aspects should also be considered when interpreting the interactions in mixed VOC systems.

745     **5.2. Yield calculation and reporting**

The representation of effectiveness of a VOC to produce SOA particle mass in a given system by its incremental yield is conceptually simple when there is only one VOC being oxidised. Equation (2) can be applied quite straightforwardly, but with consideration of the oxidant regime. There are, however, a number of considerations in the calculation and presentation of yield that should be discussed for single VOC experiments and several more that are of relevance for mixtures.

750 In Figure 3 we present a summary of the SOA particle mass in the various single VOC systems and their mixtures. It can be seen that the corrections made to account for the losses of particles to the chamber walls are substantial, with peak mass concentrations typically 30 to 40% higher than those measured, and no substantial decay after the peak mass has been formed (as expected). Whilst not without uncertainty, the loss of particles to the walls can be relatively straightforwardly estimated. This is not the case for the interactions of the walls with vapours, which has been the subject of extensive debate (Zhang et al.,

755 2014;Loza et al., 2010;Ye et al., 2016;Krechmer et al., 2020). A full discussion of this subject and characterisation of vapour interaction with the Teflon chamber walls is not provided here (fluxes to and from the chamber walls). We acknowledge that these effects will likely be substantial and that these are unquantified in our reported SOA particle mass corrections and yields. In the comparisons between different systems in our chamber, it must therefore be noted that we are implicitly assuming the vapour-wall interactions are comparable. This will introduce unquantifiable errors, since there will likely be significant vapour

760 pressure differences between products and vapour pressure dependencies of wall interactions. Most importantly, it means that, whilst the comparisons may (or may not) be valid across systems in our chamber, our reported yields are very likely not comparable with those in other chambers without further considerations. More broadly, any comparison of yields between chambers should be approached with extreme caution without full confidence that the vapour interactions with the walls of the specific chamber for the specific system have been well quantified.

765 Single value yields presented in Table 3 calculated at maximum SOA particle mass and maximum VOC consumed can provide useful classifications for comparisons of systems where temporal and mass dependence of yields are comparable. The mass

dependent curves shown in Figures 4 and 5 capture further details of the behaviour throughout the experiments and fitting the "Odum" curves to the single VOC experiments enables the "predictions" of the yields presented in the figures and as single values in Table 4 (as described in results section 4). There are a number of considerations when assessing whether it should

770     be expected that such predictions will be valid. The first of these is the inclusion of the decay of all VOCs in the yield calculation. Whether the consumption of all VOCs in a mixture should be considered in calculating the mixed yield is will depend on the question being addressed. It may be inappropriate to consider the consumption of a VOC that would not contribute to formation of SOA particles when investigating the change in yield of a VOC mixture. In the present study, and consistent with previous work, isoprene was consistently found to generate no measurable SOA particles above the background

775     chamber concentration (<1 µg m$^{-3}$) at any initial isoprene concentration and hence exhibited negligible yield. Therefore, under the conditions of our experiments, when replacing half the reactivity of a higher yield VOC with isoprene in a binary mixture, it may be considered obvious that the SOA particle mass will be reduced. This is the case in the $\alpha$-pinene / isoprene and $o$-cresol / isoprene mixtures. Instead, it may be more insightful to consider whether the yield of the $\alpha$-pinene and $o$-cresol in the binary mixtures is reduced in the presence of isoprene, using their single VOC system yields as reference. This follows the

780     approach for neutral seeded experiments in McFiggans et al. (2019). As reported in Table 4 and shown in Figure 5b), the measured binary yield is indeed below that of $\alpha$-pinene alone (either including or excluding isoprene in the calculation). For the $o$-cresol / isoprene mixture, the effect is more ambiguous, mainly because the SOA mass had not finished increasing at the conclusion of the experiments, but also because the yields are lower and deviations between the yields more difficult to measure. It should be mentioned that the particle mass yield of isoprene has been measured to be substantial in the presence

785     of acidic seeds (which were not used in our experiments) and cannot be ignored. This raises an interesting question: should there be a threshold below which the reference for mixture yield should exclude a component? Clearly a zero SOA yield component such as CO or CH$_4$ would not be expected to contribute any particle mass in a mixture and would be expected to reduce the overall mixture yield when replacing reactivity of a non-negligible yield SOA precursor. In such cases, and in the case of isoprene with a neutral seed, it appears to make sense to inspect the yield at the consumption of a known SOA precursor

790     with reference to that of the precursor for any enhancement or suppression. In mixtures of multiple VOCs with non-negligible individual particle mass yields, it makes sense to compare the particle mass yield of the mixture to the linear combination of the individual precursor's yields at the same VOC consumption. The "prediction" based on the individual precursor experimental yields is lower than the measurement in the $\alpha$-pinene / o-cresol binary mixture, possibly indicating enhancement of the mass in the mixed experiment above that which would result from the yields of the individual VOCs. The "predictions"

795     with and without isoprene consumption are comparable to the measurements in the ternary mixture. Without additional composition measurements, this could be interpreted as no interactions taking place, or possibly as the suppression of yield by the presence of isoprene offsetting the enhancement of the mass resulting from the combined oxidation of $\alpha$-pinene and $o$-cresol. However, such predictions may be oversimplistic. Clearly the oxidation conditions vary significantly across the mixtures (as seen from Figure 1 and S1) and the differences in the chemical trajectories and the time series of the ratios of

800     oxidants between the systems give reason to question the validity of the yield predictions. This is likely to be important in $\alpha$-

pinene containing systems. Here the particle mass yield from ozonolysis and OH consumption have been reported to differ substantially and Figure 6 shows that about twice as much $\alpha$-pinene results from consumption by $O_3$ as that by OH in the $\alpha$-pinene / isoprene system. In the single VOC $\alpha$-pinene system, the consumption by each oxidant was found to comprise roughly 50% of the total, based on the assumption that the consumption not attributable to the measured $O_3$ was attributable to OH (not

805    shown). A final consideration when reporting yields relates to the use of seeds as absorptive mass. Conventionally, SOA particle yield curves are plotted against absorptive mass which, in nucleation experiments, is equivalent to the SOA particle mass. In the seeded experiments in the current study, the seeds are used to provide a condensation sink to suppress nucleation, to compete effectively with the walls for condensable vapour and to facilitate measurement by ensuring particles are of a detectable size for composition measurement from early in the experiments. The seeds are nebulised from solution and

810    introduced (and presumably maintained) as metastable aqueous electrolyte solution aerosol at the RH of the experiment. It is clear that they act as absorptive mass, since organic mass is observed early in the experiments by AMS (Figure 7 and S5) and they are internally mixed throughout the experiments, as evidenced by HTDMA measurements (shown in Figure 13). Whether the total inorganic mass should be included when interpreting yield data is not clear. Figure S4 depicts the yield behaviour with the inclusion of inorganic seed in the total particle mass, assuming it acts as an effective mass for absorptive partitioning.

815    The added insight provided by such a plot is unclear, though there is a strong argument for dependence on total absorptive mass in the representation of absorptive partitioning even if this is reduced by a factor (analogous to a mass-based activity coefficient to account for non-ideal mixing effects). Note here that inorganic nitrate formation from OH oxidation of $NO_2$ and subsequent neutralisation of the $HNO_3$ by available $NH_3$ leads to the changes in inorganic components throughout the experiments as shown in the top panels of Figure 13. Effects of changing inorganic seed composition could usefully provide

820    the subject of future studies.

### 5.3. Chemical composition

The addition of measurements of particle chemical composition will provide important insights into the development of the photo-oxidation in mixtures and the resulting particle yields. Online measurements by AMS in Figures 7 and S5 indicate that

825    single VOC $o$-cresol and its binary mixture with isoprene rapidly exhibit, and then maintain through to significant particle mass production, a higher degree of oxygenation than the other systems as represented by the $f_{44}$. This contrasts sharply with the lower $f_{44}$ of all $\alpha$-pinene-containing systems. Since $\alpha$-pinene frequently dominates the mass owing to its high yield, this may offset any $o$-cresol-derived high $f_{44}$ in systems containing both $\alpha$-pinene and $o$-cresol. Clearly a less coarse diagnostic of composition is required to interrogate the reasons for the observed differences, though Shao et al. (2021a) provides more

830    insight from the high-resolution AMS analyses. The FIGAERO-CIMS data shown in Figure 8 provide an indication of the sorts of analytical products that can aid this interpretation. Whilst the additional analyses presented in Du et al. (2021) can more fully explore the impacts of the mixing of SOA precursors, several features can be directly observed from the mass

Atmospheric
Chemistry
and Physics
Discussions

Open Access

EGU

spectra. First, there is an evident increase in the contribution of higher mass ions with time in the $\alpha$-pinene single VOC system that is not observed in either the $o$-cresol single VOC system or their binary mixture. Second, there is clear evidence for signal

835    contributions from components in the mixture that are not present in the individual systems from the beginning of the experiment. This is expanded upon in Figure 9, which shows that much of the signal in analyses of the filters taken at the end of the in the ternary mixture is not found at masses corresponding to those found in individual component VOC oxidation. Such high-resolution analyses are required to unambiguously identify the specific products resulting from interactions in the system and to postulate mechanisms leading to their formation. It is not yet possible to state whether the "unique-to-mixture"

840    molecules are formed by gas phase cross-reaction, condensed phase accretion in the particles or on the filter. Neither is it currently possible to unambiguously state that this signal corresponds to the same fraction of the mass, owing to potential differential sensitivity. These aspects are discussed in detail in Shao et al. (2021b). Nonetheless, it can be stated that these compounds are only found in the mixed system. An important challenge with such identification and attributions is the requirement for substantial sampled mass. This may provide a lower limit to the yield and / or initial concentration of precursors

845    that can be studied in this way. Nevertheless, the power of such analyses is further exploited in separating the isomeric contributions to particle components as shown in Figure 10a). Combining the power of offline and online analyses, this separation of $C_7H_7NO_4$ isomers in all $o$-cresol-containing systems may be used to interpret the significant differences in the time trends of $C_7H_7NO_4$ shown in the FIGAERO-CIMS data in Figure 10b). Whilst this may be indicative of mechanistic differences, there will be confounding differences in the rate of SOA particle mass formation between the systems (and hence

850    abundance of absorptive mass) in addition to potential differences in the sensitivity in the different systems and total signal used for the normalisation because of the different FIGAERO filter loadings. These considerations are discussed in detail in Du et al. (2021) for all systems. Nonetheless, the differences in the fractional isomeric contributions and in the timeseries reveal substantial changes in the $C_7H_7NO_4$ contributions between the systems.

855    **5.4. Properties: volatility, water uptake and phase**

Figure 11 exploits the high-resolution analysis of the FIGAERO-CIMS data to present the changes in the O:C ratio of detected particle compounds as a function of their carbon number in all systems at the end of the experiments. Combining this with the ratio of signal in the particle and gas samples is used to indicate likely influences of the mixing of precursors on particle volatility. Whilst there are uncertainties associated with the partitioning, and hence volatility derivations it is evident that

860    changes in the components present in mixtures can lead to change in the volatility and potentially yield, reported in detail in Voliotis et al. (2021a, b). This is extended in Figure 12, which re-expresses the FIGAERO-CIMS data as volatility distributions, further highlighting the differences between the particle volatility in the mixture and that in the single VOC systems. This is clearly complex but is broadly consistent with the observed yield behaviour for most systems. For example, the SOA particle volatility in the single $\alpha$-pinene experiment at half reactivity is fairly similar to that measured in the binary system with

865    isoprene, consistent with their comparable yields. Similarly, the measured volatility in the α-pinene and *o*-cresol binary and in the ternary systems appear to be roughly between those obtained in the single precursor experiments, in line with the measured yields that were found to be higher than those in single *o*-cresol but equal or lower that those obtained in the single α-pinene experiments. Substantial apparent inconsistencies were found in the *o*-cresol and isoprene binary system, where the measured volatility appeared to be substantially higher than that in the single *o*-cresol system, whilst the SOA yields were somewhat

870    comparable. The reason is unclear and additional investigation might focus on reconciliation of the discrepancies between the volatility and yield behaviour in this system. Figure 13 shows the behaviour of particle water uptake and the rebound fraction of particles in an impactor in three example systems. These have been chosen for their differences in rate of formation of SOA particle mass and, in our seeded experiments, the associated organic: inorganic particle mass ratio. Clearly the rate of decrease of particle hygroscopicity and of increase of rebound fraction at higher RH follows the rate of SOA particle mass increase in

875    the system. This is a clear indication of the influence of the mixing of precursors on the change in particle properties through the change in rate of formation of condensable material (as explored in Wang et al., 2021a, b).

### 5.5. Further work

Whilst it is important to explore mixtures including multiple SOA particle precursors under controlled conditions to understand

880    behaviour in the real atmosphere, and measurements in such mixtures can reveal features inaccessible to single VOC experiment, the experimental design will determine their usefulness. Alternative and supplementary methodologies may allow more direct resolution of outstanding questions related to precursor mixing. The effects of mixed and variable oxidant concentrations throughout chamber experiments is both problematic and insightful. Clearly secondary production of oxidants (both OH and ozone) may differentially influence the decay of VOCs in the mixture and it may not be possible to scavenge

885    secondary oxidants, certainly without influencing the oxidation product distribution. In any case, secondary oxidant formation will occur in the real atmosphere and cannot be overlooked. More control over the primary oxidants may be achieved through use of "cleaner" sources, such as photolysis of $H_2O_2$. Care is required in the interpretation of condensed phase composition under the high peroxide concentrations required in such experiments, but the avoidance of $O_3$ from injection or $NO_2$ photolysis may be advantageous. Nevertheless, secondary $O_3$ will react with any unsaturated compounds present. Selection of VOCs with

890    low OH yields from ozonolysis may allow isolation of its pathways, but will limit the choice of mixtures. Augmentation of broadband illumination with discrete intense light sources such as in the JPAC chamber in the McFiggans et al. (2019) study may push up the OH:$O_3$ ratio such that the OH channels dominate, though care is necessary to avoid excessively high OH concentrations. Unless conducted at very low NOx concentrations, significant VOC consumption in batch mode chamber experiments will lead to variable VOC:NOx ratios. This will lead to variable production rate of ozone as well as changes in

895    the relative importance of the NO-mediated alkoxy radical pathways. Mechanistic interpretation of such experiments must account for these changes.  In any case, isolation of individual mechanistic pathways and probing details of kinetics and product

yields may be more suited to more targeted laboratory studies than to chamber experiments. If it is not possible to control the oxidising environment across complex mixtures, then systematic exploration of mixtures with direct and more comprehensive oxidant and peroxy radical measurements would be of benefit. Such well-instrumented studies will be able to take full advantage of the trajectories through chemical space afforded by relatively long batch mode chamber experiments. Movement towards more atmospherically representative chemical regimes would benefit from lower VOC concentration experiments. However, moving towards a more realistic radical termination regime but would present detection limit challenges to composition measurements. A more comprehensive coverage of speciated VOC and OVOC measurements using modern online mass spectrometry methods and improved resolution of such temporally resolved instruments may avoid the need to combine online and offline techniques. Whilst they reveal important impacts of the temporal changes in VOC mixtures, the batch reactor experiments in the present study are complex. Use of well-mixed flow reactor experiments to look at multiple steady states can enable focus of batch reactor experiments on sensitive areas of the chemical regime. The range of potential mixtures is not finite and so there is a need to focus on targeted areas of importance. It is not immediately obvious how this should be done, though it should be remembered that oxidation and SOA formation will occur during both day and night and mixed night-time oxidation by $NO_3$ should not be forgotten.

## 6. Conclusions

A comprehensive suite of instrumentation was deployed to investigate the formation of SOA particulate mass on inorganic seeds in chamber photo-oxidation of anthropogenic (o-cresol) and biogenic (α-pinene and isoprene) VOCs and their binary and ternary mixtures in the presence of NOx. Whilst compromises were necessary in the experimental design and the complexity of the systems introduced substantial challenges to their interpretation, a number of important observations were possible.

First, the photochemical trajectory is understandably system dependent and the rates of consumption of each VOC by each oxidant consequently variable.

Second, the yield concept typically used for an individual VOC requires careful consideration when adapting it for use with complex mixtures. In order to account for the dependence of condensed mass on available adsorptive mass, it will be necessary to use the individual component yield at the same mass as in the mixtures. However, in order to compare the mass formed at the same VOC consumption, it is necessary to reference this to the corresponding single precursor experiment at that same VOC consumption and therefore not that calculated at the same adsorptive mass.

In mixtures where the majority of the mass is contributed by only one component precursor, it is possible to identify the existence of, and quantify, any interactions in terms of SOA mass or yield. Thus, as shown in Figure 5 there is clear indication

of suppression of the yield of α-pinene in its mixture with isoprene, but as with the *o*-cresol / isoprene mixture there is a possible indication of enhancement, though this is too small to be unambiguous.

It is straightforward to make a comparison between the predicted and measured yield in mixtures of precursors both with appreciable yield. It is straightforward to make a comparison between the measured yield of single components with its yield

930     in a mixture with a precursor of zero yield. Where two components with appreciable yield are mixed with another VOC with no yield the reference point for the comparison is complex.

The mixed α-pinene / *o*-cresol system is measured to have enhanced yield above that expected from additivity of the individual VOC yield at the same consumption. In such mixtures, where there is a significant contribution to the SOA mass from more than one component precursor, we are unable to unambiguously attribute any discrepancies in predicted and measured mass

935     to physical or chemical interactions. This is because yield and partitioned mass will depend both on available adsorptive mass and upon the rate of consumption of individual VOC and production of condensable oxidation products. In the ternary system, the measured yield is comparable to that calculated from additivity of the component yields. It is unclear whether this is attributable to cancelling of suppression and enhancement effects, but chemical interactions are evident from the unique-to mixture components.

940     The trajectories of physical properties such as water uptake and phase behaviour of the particles will depend on the rates of formation of SOA particle mass, so changes in these rates in mixtures will control changes in particle physical properties.

Mixing experiments are crucial and highly beneficial for our understanding on atmospheric chemical interactions. However, the interpretation quickly becomes complex and both the experimental design and evaluation needs to be scrutinised carefully. Here, advanced online and offline compositional measurements can reveal substantial additional information to aid in the

945     interpretation of yield data, including components uniquely found in mixtures and physicochemical property changes in the SOA formed from mixtures of VOCs.

Atmospheric
Chemistry
and Physics
Discussions

955 Atmospheric Measurement and Observational Facility (AMOF). We acknowledge Dr. Zhijun Wu from Peking University, China, for providing Bounce behaviour instrument through Trans-National Access (TNA) of EUROCHAMP-2020. MH and TFM acknowledge the strategic research area MERGE, the Swedish Research Council (grant number 2018-04430), the Formas (grant number 2019-586). TFM acknowledges the support from the EU Project FORCeS (grant agreement no. 821205).

**Competing interests**

960 The authors declare that they have no conflict of interest

**Author contributions**

GM, MRA, MH, TFM AV, YW, YS and MD conceived the study. AV, YW, YS and MD conducted the experiments and data analysis. TJB, DH and KP provided on-site support with the instrument deployment and data analysis procedures. JFH provided scientific advice. GM, AV, YW, YS and MD wrote the manuscript with inputs from all co-authors.

965 **Data Availability**

All the data used in this study are available upon request from the corresponding author(s)

**References**

Alfarra, M. R., Hamilton, J. F., Wyche, K. P., Good, N., Ward, M. W., Carr, T., Barley, M. H., Monks, P. S., Jenkin, M. E.,
970 Lewis, A. C., and McFiggans, G. B.: The effect of photochemical ageing and initial precursor concentration on the composition and hygroscopic properties of β-caryophyllene secondary organic aerosol, Atmos. Chem. Phys., 12, 6417-6436, 10.5194/acp-12-6417-2012, 2012.

Alfarra, M. R., Good, N., Wyche, K. P., Hamilton, J. F., Monks, P. S., Lewis, A. C., and McFiggans, G.: Water uptake is independent of the inferred composition of secondary aerosols derived from multiple biogenic VOCs, Atmos. Chem. Phys.,
975 13, 11769-11789, 10.5194/acp-13-11769-2013, 2013.

Atkinson, R., Baulch, D. L., Cox, R. A., Crowley, J. N., Hampson, R. F., Hynes, R. G., Jenkin, M. E., Rossi, M. J., Troe, J., and Subcommittee, I.: Evaluated kinetic and photochemical data for atmospheric chemistry: Volume II &ndash; gas phase reactions of organic species, Atmos. Chem. Phys., 6, 3625-4055, 10.5194/acp-6-3625-2006, 2006.

Aumont, B., Szopa, S., and Madronich, S.: Modelling the evolution of organic carbon during its gas-phase tropospheric
980 oxidation: development of an explicit model based on a self generating approach, Atmos. Chem. Phys., 5, 2497-2517, 10.5194/acp-5-2497-2005, 2005.

Bannan, T. J., Le Breton, M., Priestley, M., Worrall, S. D., Bacak, A., Marsden, N. A., Mehra, A., Hammes, J., Hallquist, M., Alfarra, M. R., Krieger, U. K., Reid, J. P., Jayne, J., Robinson, W., McFiggans, G., Coe, H., Percival, C. J., and Topping, D.:

A method for extracting calibrated volatility information from the FIGAERO-HR-ToF-CIMS and its experimental application, Atmos Meas Tech, 12, 1429-1439, 10.5194/amt-12-1429-2019, 2019.

Berndt, T., Richters, S., Jokinen, T., Hyttinen, N., Kurtén, T., Otkjær, R. V., Kjaergaard, H. G., Stratmann, F., Herrmann, H., Sipilä, M., Kulmala, M., and Ehn, M.: Hydroxyl radical-induced formation of highly oxidized organic compounds, Nature Communications, 7, 13677, 10.1038/ncomms13677, 2016.

Berndt, T., Mentler, B., Scholz, W., Fischer, L., Herrmann, H., Kulmala, M., and Hansel, A.: Accretion Product Formation from Ozonolysis and OH Radical Reaction of α-Pinene: Mechanistic Insight and the Influence of Isoprene and Ethylene, Environmental Science & Technology, 52, 11069-11077, 10.1021/acs.est.8b02210, 2018.

Bianchi, F., Kurten, T., Riva, M., Mohr, C., Rissanen, M. P., Roldin, P., Berndt, T., Crounse, J. D., Wennberg, P. O., Mentel, T. F., Wildt, J., Junninen, H., Jokinen, T., Kulmala, M., Worsnop, D. R., Thornton, J. A., Donahue, N., Kjaergaard, H. G., and Ehn, M.: Highly Oxygenated Organic Molecules (HOM) from Gas-Phase Autoxidation Involving Peroxy Radicals: A Key Contributor to Atmospheric Aerosol, Chem Rev, 119, 3472-3509, 10.1021/acs.chemrev.8b00395, 2019.

Carlton, A. G., Wiedinmyer, C., and Kroll, J. H.: A review of Secondary Organic Aerosol (SOA) formation from isoprene, Atmos. Chem. Phys., 9, 4987-5005, 10.5194/acp-9-4987-2009, 2009.

Cash, J. M., Heal, M. R., Langford, B., and Drewer, J.: A review of stereochemical implications in the generation of secondary organic aerosol from isoprene oxidation, Environmental Science: Processes & Impacts, 18, 1369-1380, 10.1039/C6EM00354K, 2016.

Charan, S. M., Huang, Y., and Seinfeld, J. H.: Computational Simulation of Secondary Organic Aerosol Formation in Laboratory Chambers, Chem Rev, 119, 11912-11944, 10.1021/acs.chemrev.9b00358, 2019.

Cohen, A. J., Brauer, M., Burnett, R., Anderson, H. R., Frostad, J., Estep, K., Balakrishnan, K., Brunekreef, B., Dandona, L., Dandona, R., Feigin, V., Freedman, G., Hubbell, B., Jobling, A., Kan, H., Knibbs, L., Liu, Y., Martin, R., Morawska, L., Pope, C. A., III, Shin, H., Straif, K., Shaddick, G., Thomas, M., van Dingenen, R., van Donkelaar, A., Vos, T., Murray, C. J. L., and Forouzanfar, M. H.: Estimates and 25-year trends of the global burden of disease attributable to ambient air pollution: an analysis of data from the Global Burden of Diseases Study 2015, The Lancet, 389, 1907-1918, 10.1016/S0140-6736(17)30505-6, 2017.

Cox, R. A., Ammann, M., Crowley, J. N., Herrmann, H., Jenkin, M. E., McNeill, V. F., Mellouki, A., Troe, J., and Wallington, T. J.: Evaluated kinetic and photochemical data for atmospheric chemistry: Volume VII – Criegee intermediates, Atmos. Chem. Phys., 20, 13497–13519, https://doi.org/10.5194/acp-20-13497-2020, 2020

Crounse, J. D., Nielsen, L. B., Jørgensen, S., Kjaergaard, H. G., and Wennberg, P. O.: Autoxidation of Organic Compounds in the Atmosphere, The Journal of Physical Chemistry Letters, 4, 3513-3520, 10.1021/jz4019207, 2013.

Donahue, N. M., Robinson, A. L., Stanier, C. O., and Pandis, S. N.: Coupled partitioning, dilution, and chemical aging of semivolatile organics, Environmental Science & Technology, 40, 2635-2643, 2006.

Donahue, N. M., Epstein, S. A., Pandis, S. N., and Robinson, A. L.: A two-dimensional volatility basis set: 1. organic-aerosol mixing thermodynamics, Atmos. Chem. Phys., 11, 3303-3318, 10.5194/acp-11-3303-2011, 2011.

Donahue, N. M., Henry, K. M., Mentel, T. F., Kiendler-Scharr, A., Spindler, C., Bohn, B., Brauers, T., Dorn, H. P., Fuchs, H., Tillmann, R., Wahner, A., Saathoff, H., Naumann, K.-H., Möhler, O., Leisner, T., Müller, L., Reinnig, M.-C., Hoffmann, T., Salo, K., Hallquist, M., Frosch, M., Bilde, M., Tritscher, T., Barmet, P., Praplan, A. P., DeCarlo, P. F., Dommen, J., Prévôt, A. S. H., and Baltensperger, U.: Aging of biogenic secondary organic aerosol via gas-phase OH radical reactions, 109, 13503-13508, 10.1073/pnas.1115186109 %J Proceedings of the National Academy of Sciences, 2012.

Du, M., Voliotis, A., Shao, Y., Wang, Y., Bannan, T. J., Pereira, K., Hamilton J. F., Percival C. J., Alfarra, M. R., McFiggans, G.: Combined application of on-line FIGAERO-CIMS and off-line Orbitrap LC-MS to characterize the chemical composition
1025     of SOA in smog chamber studies. In preparation for Atmos. Chem. Phys. Discuss., 2021a

Ehn, M., Kleist, E., Junninen, H., Petäjä, T., Lönn, G., Schobesberger, S., Dal Maso, M., Trimborn, A., Kulmala, M., Worsnop, D. R., Wahner, A., Wildt, J., and Mentel, T. F.: Gas phase formation of extremely oxidized pinene reaction products in chamber and ambient air, Atmos. Chem. Phys., 12, 5113-5127, 10.5194/acp-12-5113-2012, 2012.

Ehn, M., Thornton, J. A., Kleist, E., Sipilä, M., Junninen, H., Pullinen, I., Springer, M., Rubach, F., Tillmann, R., Lee, B.,
1030     Lopez-Hilfiker, F., Andres, S., Acir, I.-H., Rissanen, M., Jokinen, T., Schobesberger, S., Kangasluoma, J., Kontkanen, J., Nieminen, T., Kurtén, T., Nielsen, L. B., Jørgensen, S., Kjaergaard, H. G., Canagaratna, M., Maso, M. D., Berndt, T., Petäjä, T., Wahner, A., Kerminen, V.-M., Kulmala, M., Worsnop, D. R., Wildt, J., and Mentel, T. F.: A large source of low-volatility secondary organic aerosol, Nature, 506, 476-479, 10.1038/nature13032, 2014.

Emanuelsson, E. U., Hallquist, M., Kristensen, K., Glasius, M., Bohn, B., Fuchs, H., Kammer, B., Kiendler-Scharr, A., Nehr,
1035     S., Rubach, F., Tillmann, R., Wahner, A., Wu, H. C., and Mentel, T. F.: Formation of anthropogenic secondary organic aerosol (SOA) and its influence on biogenic SOA properties, Atmos. Chem. Phys., 13, 2837-2855, 10.5194/acp-13-2837-2013, 2013.

Garmash, O., Rissanen, M. P., Pullinen, I., Schmitt, S., Kausiala, O., Tillmann, R., Zhao, D., Percival, C., Bannan, T. J., Priestley, M., Hallquist, Å. M., Kleist, E., Kiendler-Scharr, A., Hallquist, M., Berndt, T., McFiggans, G., Wildt, J., Mentel, T. F., and Ehn, M.: Multi-generation OH oxidation as a source for highly oxygenated organic molecules from aromatics, Atmos.
1040     Chem. Phys., 20, 515-537, 10.5194/acp-20-515-2020, 2020.

Goldstein, A. H., and Galbally, I. E.: Known and unexplored organic constituents in the earth's atmosphere, Environmental Science & Technology, 41, 1514-1521, 2007.

Good, N., Coe, H., and McFiggans, G.: Instrumentational operation and analytical methodology for the reconciliation of aerosol water uptake under sub- and supersaturated conditions, Atmos. Meas. Tech., 3, 1241-1254, 10.5194/amt-3-1241-2010,
1045     2010.

Hallquist, M., Wenger, J. C., Baltensperger, U., Rudich, Y., Simpson, D., Claeys, M., Dommen, J., Donahue, N. M., George, C., Goldstein, A. H., Hamilton, J. F., Herrmann, H., Hoffmann, T., Iinuma, Y., Jang, M., Jenkin, M. E., Jimenez, J. L., Kiendler-Scharr, A., Maenhaut, W., McFiggans, G., Mentel, T. F., Monod, A., Prévôt, A. S. H., Seinfeld, J. H., Surratt, J. D., Szmigielski, R., and Wildt, J.: The formation, properties and impact of secondary organic aerosol: current and emerging issues, Atmos.
1050     Chem. Phys., 9, 5155-5236, 10.5194/acp-9-5155-2009, 2009.

Hamilton, J. F., Alfarra, M. R., Wyche, K. P., Ward, M. W., Lewis, A. C., McFiggans, G. B., Good, N., Monks, P. S., Carr, T., White, I. R., and Purvis, R. M.: Investigating the use of secondary organic aerosol as seed particles in simulation chamber experiments, Atmospheric Chemistry and Physics, 11, 5917-5929, 10.5194/acp-11-5917-2011, 2011.

Hao, L. Q., Yli-Pirilä, P., Tiitta, P., Romakkaniemi, S., Vaattovaara, P., Kajos, M. K., Rinne, J., Heijari, J., Kortelainen, A.,
1055     Miettinen, P., Kroll, J. H., Holopainen, J. K., Smith, J. N., Joutsensaari, J., Kulmala, M., Worsnop, D. R., and Laaksonen, A.: New particle formation from the oxidation of direct emissions of pine seedlings, Atmos. Chem. Phys., 9, 8121-8137, 10.5194/acp-9-8121-2009, 2009.

IPCC: Climate Change 2013: The Physical Science Basis. Contribution of Working Group I to the Fifth Assessment Report of the Intergovernmental Panel on Climate Change, Cambridge University Press, Cambridge, United Kingdom and New York,
1060     NY, USA, 1535 pp., 2013.

IPCC: Global Warming of 1.5oC

IPCC, 2018: Summary for Policymakers. In: Global warming of 1.5&deg;C. An IPCC Special Report on the impacts of global warming of 1.5&deg;C above pre-industrial levels and related global greenhouse gas emission pathways,in the context of strengthening the global response to the threat of climate change, sustainable development, and efforts to eradicate poverty, World Meteorological Organization, 2018.

Jaoui, M., and Kamens, R. M.: Gaseous and Particulate Oxidation Products Analysis of a Mixture of α-pinene + β-pinene/O3/Air in the Absence of Light and α-pinene + β-pinene/NOx/Air in the Presence of Natural Sunlight, Journal of Atmospheric Chemistry, 44, 259-297, 10.1023/A:1022977427523, 2003.

Jenkin, M. E., Wyche, K. P., Evans, C. J., Carr, T., Monks, P. S., Alfarra, M. R., Barley, M. H., McFiggans, G. B., Young, J. C., and Rickard, A. R.: Development and chamber evaluation of the MCM v3.2 degradation scheme for β-caryophyllene, Atmos. Chem. Phys., 12, 5275-5308, 10.5194/acp-12-5275-2012, 2012.

Jokinen, T., Berndt, T., Makkonen, R., Kerminen, V.-M., Junninen, H., Paasonen, P., Stratmann, F., Herrmann, H., Guenther, A. B., Worsnop, D. R., Kulmala, M., Ehn, M., and Sipilä, M.: Production of extremely low volatile organic compounds from biogenic emissions: Measured yields and atmospheric implications, 112, 7123-7128, 10.1073/pnas.1423977112 %J Proceedings of the National Academy of Sciences, 2015.

Joutsensaari, J., Loivamäki, M., Vuorinen, T., Miettinen, P., Nerg, A. M., Holopainen, J. K., and Laaksonen, A.: Nanoparticle formation by ozonolysis of inducible plant volatiles, Atmos. Chem. Phys., 5, 1489-1495, 10.5194/acp-5-1489-2005, 2005.

Kaltsonoudis, C., Kostenidou, E., Louvaris, E., Psichoudaki, M., Tsiligiannis, E., Florou, K., Liangou, A., and Pandis, S. N.: Characterization of fresh and aged organic aerosol emissions from meat charbroiling, Atmos. Chem. Phys., 17, 7143-7155, 10.5194/acp-17-7143-2017, 2017.

Kanakidou, M., Seinfeld, J. H., Pandis, S. N., Barnes, I., Dentener, F. J., Facchini, M. C., Van Dingenen, R., Ervens, B., Nenes, A., Nielsen, C. J., Swietlicki, E., Putaud, J. P., Balkanski, Y., Fuzzi, S., Horth, J., Moortgat, G. K., Winterhalter, R., Myhre, C. E. L., Tsigaridis, K., Vignati, E., Stephanou, E. G., and Wilson, J.: Organic aerosol and global climate modelling: a review, Atmos. Chem. Phys., 5, 1053-1123, 10.5194/acp-5-1053-2005, 2005.

Kiendler-Scharr, A., Wildt, J., Maso, M. D., Hohaus, T., Kleist, E., Mentel, T. F., Tillmann, R., Uerlings, R., Schurr, U., and Wahner, A.: New particle formation in forests inhibited by isoprene emissions, Nature, 461, 381-384, 10.1038/nature08292, 2009.

Krechmer, J. E., Day, D. A., and Jimenez, J. L.: Always Lost but Never Forgotten: Gas-Phase Wall Losses Are Important in All Teflon Environmental Chambers, Environmental Science & Technology, 54, 12890-12897, 10.1021/acs.est.0c03381, 2020.

Leighton, P. A.: Photochemistry of air pollution, 9, Phys. Chem., 300 pp., 1961.

Liu, Y., Wu, Z., Wang, Y., Xiao, Y., Gu, F., Zheng, J., Tan, T., Shang, D., Wu, Y., Zeng, L., Hu, M., Bateman, A. P., and Martin, S. T.: Submicrometer Particles Are in the Liquid State during Heavy Haze Episodes in the Urban Atmosphere of Beijing, China, Environ Sci Tech Let, 4, 427-432, 10.1021/acs.estlett.7b00352, 2017.

Loza, C. L., Chan, A. W. H., Galloway, M. M., Keutsch, F. N., Flagan, R. C., and Seinfeld, J. H.: Characterization of Vapor Wall Loss in Laboratory Chambers, Environmental Science & Technology, 44, 5074-5078, 10.1021/es100727v, 2010.

McFiggans, G., Coe, H., Burgess, R., Allan, J., Cubison, M., Alfarra, M. R., Saunders, R., Saiz-Lopez, A., Plane, J. M. C., Wevill, D., Carpenter, L., Rickard, A. R., and Monks, P. S.: Direct evidence for coastal iodine particles from Laminaria macroalgae – linkage to emissions of molecular iodine, Atmos. Chem. Phys., 4, 701-713, 10.5194/acp-4-701-2004, 2004.

45

Atmospheric
Chemistry
and Physics
Discussions

1100   McFiggans, G., Mentel, T. F., Wildt, J., Pullinen, I., Kang, S., Kleist, E., Schmitt, S., Springer, M., Tillmann, R., Wu, C., Zhao, D., Hallquist, M., Faxon, C., Le Breton, M., Hallquist, A. M., Simpson, D., Bergstrom, R., Jenkin, M. E., Ehn, M., Thornton, J. A., Alfarra, M. R., Bannan, T. J., Percival, C. J., Priestley, M., Topping, D., and Kiendler-Scharr, A.: Secondary organic aerosol reduced by mixture of atmospheric vapours, Nature, 565, 587-593, 10.1038/s41586-018-0871-y, 2019.

Mehra, A., Wang, Y., Krechmer, J. E., Lambe, A., Majluf, F., Morris, M. A., Priestley, M., Bannan, T. J., Bryant, D. J., Pereira,
1105   K. L., Hamilton, J. F., Rickard, A. R., Newland, M. J., Stark, H., Croteau, P., Jayne, J. T., Worsnop, D. R., Canagaratna, M. R., Wang, L., and Coe, H.: Evaluation of the chemical composition of gas- and particle-phase products of aromatic oxidation, Atmos. Chem. Phys., 20, 9783-9803, 10.5194/acp-20-9783-2020, 2020.

Mellouki, A., Ammann, M., Cox, R. A., Crowley, J. N., Herrmann, H., Jenkin, M. E., McNeill, V. F., Troe, J., and Wallington, T. J.: Evaluated kinetic and photochemical data for atmospheric chemistry: volume VIII – gas-phase reactions of organic
1110   species with four, or more, carbon atoms ($\geq$  C4), Atmos. Chem. Phys., 21, 4797-4808, 10.5194/acp-21-4797-2021, 2021.

Mentel, T. F., Wildt, J., Kiendler-Scharr, A., Kleist, E., Tillmann, R., Dal Maso, M., Fisseha, R., Hohaus, T., Spahn, H., Uerlings, R., Wegener, R., Griffiths, P. T., Dinar, E., Rudich, Y., and Wahner, A.: Photochemical production of aerosols from real plant emissions, Atmos. Chem. Phys., 9, 4387-4406, 10.5194/acp-9-4387-2009, 2009.

1115   Molteni, U., Bianchi, F., Klein, F., El Haddad, I., Frege, C., Rossi, M. J., Dommen, J., and Baltensperger, U.: Formation of highly oxygenated organic molecules from aromatic compounds, Atmos. Chem. Phys., 18, 1909-1921, 10.5194/acp-18-1909-2018, 2018.

Nakao, S., Shrivastava, M., Nguyen, A., Jung, H., and Cocker, D.: Interpretation of Secondary Organic Aerosol Formation from Diesel Exhaust Photooxidation in an Environmental Chamber, Aerosol Sci Tech, 45, 964-972,
1120   10.1080/02786826.2011.573510, 2011.

Nakao, S., Liu, Y., Tang, P., Chen, C. L., Zhang, J., and Cocker Iii, D. R.: Chamber studies of SOA formation from aromatic hydrocarbons: observation of limited glyoxal uptake, Atmos. Chem. Phys., 12, 3927-3937, 10.5194/acp-12-3927-2012, 2012.

Ng, N. L., Canagaratna, M. R., Zhang, Q., Jimenez, J. L., Tian, J., Ulbrich, I. M., Kroll, J. H., Docherty, K. S., Chhabra, P. S., Bahreini, R., Murphy, S. M., Seinfeld, J. H., Hildebrandt, L., Donahue, N. M., DeCarlo, P. F., Lanz, V. A., Prévôt, A. S. H.,
1125   Dinar, E., Rudich, Y., and Worsnop, D. R.: Organic aerosol components observed in Northern Hemispheric datasets from Aerosol Mass Spectrometry, Atmos. Chem. Phys., 10, 4625-4641, 10.5194/acp-10-4625-2010, 2010.

Nordin, E. Z., Eriksson, A. C., Roldin, P., Nilsson, P. T., Carlsson, J. E., Kajos, M. K., Hellén, H., Wittbom, C., Rissler, J., Löndahl, J., Swietlicki, E., Svenningsson, B., Bohgard, M., Kulmala, M., Hallquist, M., and Pagels, J. H.: Secondary organic aerosol formation from idling gasoline passenger vehicle emissions investigated in a smog chamber, Atmos. Chem. Phys., 13,
1130   6101-6116, 10.5194/acp-13-6101-2013, 2013.

Odum, J. R., Hoffmann, T., Bowman, F., Collins, D., Flagan, R. C., and Seinfeld, J. H.: Gas/Particle Partitioning and Secondary Organic Aerosol Yields, Environmental Science & Technology, 30, 2580-2585, 10.1021/es950943+, 1996.

Pankow, J. F.: An absorption-model of gas-particle partitioning of organic-compounds in the atmosphere, Atmos. Environ., 28, 185–188, 10.1016/1352-2310(94)90093-0, 1994.

1135   Pinto, D. M., Tiiva, P., Miettinen, P., Joutsensaari, J., Kokkola, H., Nerg, A.-M., Laaksonen, A., and Holopainen, J. K.: The effects of increasing atmospheric ozone on biogenic monoterpene profiles and the formation of secondary aerosols, Atmos Environ, 41, 4877-4887, 10.1016/j.atmosenv.2007.02.006, 2007.

Platt, S. M., El Haddad, I., Zardini, A. A., Clairotte, M., Astorga, C., Wolf, R., Slowik, J. G., Temime-Roussel, B., Marchand, N., Ježek, I., Drinovec, L., Močnik, G., Möhler, O., Richter, R., Barmet, P., Bianchi, F., Baltensperger, U., and Prévôt, A. S.

1140     H.: Secondary organic aerosol formation from gasoline vehicle emissions in a new mobile environmental reaction chamber, Atmos. Chem. Phys., 13, 9141-9158, 10.5194/acp-13-9141-2013, 2013.

Priestley, M., Bannan, T. J., Le Breton, M., Worrall, S. D., Kang, S., Pullinen, I., Schmitt, S., Tillmann, R., Kleist, E., Zhao, D., Wildt, J., Garmash, O., Mehra, A., Bacak, A., Shallcross, D. E., Kiendler-Scharr, A., Hallquist, Å. M., Ehn, M., Coe, H., Percival, C. J., Hallquist, M., Mentel, T. F., and McFiggans, G.: Chemical characterisation of benzene oxidation products
1145     under high- and low-NOx conditions using chemical ionisation mass spectrometry, Atmos. Chem. Phys., 21, 3473-3490, 10.5194/acp-21-3473-2021, 2021.

Pullinen, I., Schmitt, S., Kang, S., Sarrafzadeh, M., Schlag, P., Andres, S., Kleist, E., Mentel, T. F., Rohrer, F., Springer, M., Tillmann, R., Wildt, J., Wu, C., Zhao, D., Wahner, A., and Kiendler-Scharr, A.: Impact of NOx on secondary organic aerosol (SOA) formation from α-pinene and β-pinene photooxidation: the role of highly oxygenated organic nitrates, Atmos. Chem.
1150     Phys., 20, 10125–10147, https://doi.org/10.5194/acp-20-10125-2020, 2020.

Reyes-Villegas, E., Bannan, T., Le Breton, M., Mehra, A., Priestley, M., Percival, C., Coe, H., and Allan, J. D.: Online Chemical Characterization of Food-Cooking Organic Aerosols: Implications for Source Apportionment, Environmental Science & Technology, 52, 5308-5318, 10.1021/acs.est.7b06278, 2018.

Rohrer, F., Bohn, B., Brauers, T., Brüning, D., Johnen, F. J., Wahner, A., and Kleffmann, J.: Characterisation of the photolytic

1155     HONO-source in the atmosphere simulation chamber SAPHIR, Atmos. Chem. Phys., 5, 2189-2201, 10.5194/acp-5-2189-2005, 2005.

Sarrafzadeh, M., Wildt, J., Pullinen, I., Springer, M., Kleist, E., Tillmann, R., Schmitt, S. H., Wu, C., Mentel, T. F., Zhao, D., Hastie, D. R., and Kiendler-Scharr, A.: Impact of NOx and OH on secondary organic aerosol formation from β-pinene photooxidation, Atmos. Chem. Phys., 16, 11237–11248, 10.5194/acp-16-11237-2016, 2016.

1160     Schervish, M., and Donahue, N. M.: Peroxy radical chemistry and the volatility basis set, Atmos. Chem. Phys., 20, 1183-1199, 10.5194/acp-20-1183-2020, 2020.

Schwantes, R. H., Schilling, K. A., McVay, R. C., Lignell, H., Coggon, M. M., Zhang, X., Wennberg, P. O., and Seinfeld, J. H.: Formation of highly oxygenated low-volatility products from cresol oxidation, Atmospheric Chemistry and Physics, 17, 3453-3474, 10.5194/acp-17-3453-2017, 2017.

1165     Shao, Y., Wang, Y., Du, M., Voliotis, A., Alfarra, M. R., Turner, S. F., and McFiggans, G.: Characterisation of the Manchester Aerosol Chamber facility, Atmos. Meas. Tech. Discuss., 2021, 1-50, 10.5194/amt-2021-147, 2021a.

Shao, Y., Voliotis, A., Du, M., Wang, Y., Pereira, K., Hamilton, J., Alfarra, M. R., McFiggans, G.: Chemical composition of secondary organic aerosol particles formed from mixtures of anthropogenic and biogenic precursors. In preparation for Atmos. Chem. Phys. Discuss., 2021b.

1170     Shao, Y., Voliotis, A., Du, M., Wang, Y., Pereira, K., Hamilton, J., Alfarra, M. R., McFiggans, G.: Characterisation of the oxidation state of secondary organic aerosols in mixed precursor systems. In preparation for Atmos. Chem. Phys. Discuss., 2021c.

Shilling, J. E., Zawadowicz, M. A., Liu, J. M., Zaveri, R. A., and Zelenyuk, A.: Photochemical Aging Alters Secondary Organic Aerosol Partitioning Behavior, Acs Earth Space Chem, 3, 2704-2716, 10.1021/acsearthspacechem.9b00248, 2019.

1175     Shrivastava, M., Cappa, C. D., Fan, J., Goldstein, A. H., Guenther, A. B., Jimenez, J. L., Kuang, C., Laskin, A., Martin, S. T., Ng, N. L., Petaja, T., Pierce, J. R., Rasch, P. J., Roldin, P., Seinfeld, J. H., Shilling, J., Smith, J. N., Thornton, J. A., Volkamer, R., Wang, J., Worsnop, D. R., Zaveri, R. A., Zelenyuk, A., and Zhang, Q.: Recent advances in understanding secondary organic aerosol: Implications for global climate forcing, 55, 509-559, 10.1002/2016rg000540, 2017.

Spracklen, D. V., Jimenez, J. L., Carslaw, K. S., Worsnop, D. R., Evans, M. J., Mann, G. W., Zhang, Q., Canagaratna, M. R.,
1180    Allan, J., Coe, H., McFiggans, G., Rap, A., and Forster, P.: Aerosol mass spectrometer constraint on the global secondary
organic aerosol budget, Atmos. Chem. Phys., 11, 12109-12136, 10.5194/acp-11-12109-2011, 2011.

Thornton, J. A., Shilling, J. E., Shrivastava, M., D'Ambro, E. L., Zawadowicz, M. A., and Liu, J.: A Near-Explicit Mechanistic
Evaluation of Isoprene Photochemical Secondary Organic Aerosol Formation and Evolution: Simulations of Multiple Chamber
Experiments with and without Added NOx, Acs Earth Space Chem, 4, 1161-1181, 10.1021/acsearthspacechem.0c00118, 2020.

1185    Tiitta, P., Leskinen, A., Hao, L., Yli-Pirilä, P., Kortelainen, M., Grigonyte, J., Tissari, J., Lamberg, H., Hartikainen, A.,
Kuuspalo, K., Kortelainen, A. M., Virtanen, A., Lehtinen, K. E. J., Komppula, M., Pieber, S., Prévôt, A. S. H., Onasch, T. B.,
Worsnop, D. R., Czech, H., Zimmermann, R., Jokiniemi, J., and Sippula, O.: Transformation of logwood combustion emissions
in a smog chamber: formation of secondary organic aerosol and changes in the primary organic aerosol upon daytime and
nighttime aging, Atmos. Chem. Phys., 16, 13251-13269, 10.5194/acp-16-13251-2016, 2016.

1190    Tsigaridis, K., and Kanakidou, M.: The Present and Future of Secondary Organic Aerosol Direct Forcing on Climate, Current
Climate Change Reports, 4, 84-98, 10.1007/s40641-018-0092-3, 2018.

Tsiligiannis, E., Hammes, J., Salvador, C. M., Mentel, T. F., and Hallquist, M.: Effect of NOx on 1,3,5-trimethylbenzene
(TMB) oxidation product distribution and particle formation, Atmos. Chem. Phys., 19, 15073-15086, 10.5194/acp-19-15073-
2019, 2019.

1195    VanReken, T. M., Greenberg, J. P., Harley, P. C., Guenther, A. B., and Smith, J. N.: Direct measurement of particle formation
and growth from the oxidation of biogenic emissions, Atmos. Chem. Phys., 6, 4403-4413, 10.5194/acp-6-4403-2006, 2006.

Voliotis, A., Wang, Y., Shao, Y., Du, M., Bannan, T. J., Percival, C. J., Pandis, S. N., Alfarra, M. R., and McFiggans, G.:
Exploring the composition and volatility of secondary organic aerosols in mixed anthropogenic and biogenic precursor
systems, Atmos. Chem. Phys., 21, 14251-14273, 2021a

1200    Voliotis, A., Wang, Y., Shao, Y., Du, M., Bannan, T. J., Percival, C. J., Pandis, S. N., Alfarra, M. R., and McFiggans, G.: The
influence of the addition of a reactive low SOA yield VOC on the volatility of particles formed from photo-oxidation of
anthropogenic – biogenic mixtures, in prep for Atmos. Chem. Phys. Discuss., 2021b

Wang, S., Wu, R., Berndt, T., Ehn, M., and Wang, L.: Formation of Highly Oxidized Radicals and Multifunctional Products
from the Atmospheric Oxidation of Alkylbenzenes, Environmental Science & Technology, 51, 8442-8449,
1205    10.1021/acs.est.7b02374, 2017.

Wang, Y., Mehra, A., Krechmer, J. E., Yang, G., Hu, X., Lu, Y., Lambe, A., Canagaratna, M., Chen, J., Worsnop, D., Coe,
H., and Wang, L.: Oxygenated products formed from OH-initiated reactions of trimethylbenzene: autoxidation and accretion,
Atmos. Chem. Phys., 20, 9563-9579, 10.5194/acp-20-9563-2020, 2020.

Weitkamp, E. A., Sage, A. M., Pierce, J. R., Donahue, N. M., and Robinson, A. L.: Organic Aerosol Formation from
1210    Photochemical Oxidation of Diesel Exhaust in a Smog Chamber, Environmental Science & Technology, 41, 6969-6975,
10.1021/es070193r, 2007.

Whalley, L. K., Stone, D., Bandy, B., Dunmore, R., Hamilton, J. F., Hopkins, J., Lee, J. D., Lewis, A. C., and Heard, D. E.:
Atmospheric OH reactivity in central London: observations, model predictions and estimates of in situ ozone production,
Atmos. Chem. Phys., 16, 2109-2122, 10.5194/acp-16-2109-2016, 2016.

1215    Wyche, K. P., Ryan, A. C., Hewitt, C. N., Alfarra, M. R., McFiggans, G., Carr, T., Monks, P. S., Smallbone, K. L., Capes, G.,
Hamilton, J. F., Pugh, T. A. M., and MacKenzie, A. R.: Emissions of biogenic volatile organic compounds and subsequent
photochemical production of secondary organic aerosol in mesocosm studies of temperate and tropical plant species, Atmos.
Chem. Phys., 14, 12781-12801, 10.5194/acp-14-12781-2014, 2014.

Ye, P., Ding, X., Hakala, J., Hofbauer, V., Robinson, E. S., and Donahue, N. M.: Vapor wall loss of semi-volatile organic compounds in a Teflon chamber, Aerosol Sci Tech, 50, 822-834, 10.1080/02786826.2016.1195905, 2016.

Zhang, X., Cappa, C. D., Jathar, S. H., Mcvay, R. C., Ensberg, J. J., Kleeman, M. J., and Seinfeld, J. H.: Influence of vapor wall loss in laboratory chambers on yields of secondary organic aerosol, P Natl Acad Sci USA, 111, 5802-5807, 10.1073/pnas.1404727111, 2014.

Ziemann, P. J., and Atkinson, R.: Kinetics, products, and mechanisms of secondary organic aerosol formation, Chemical Society Reviews, 41, 6582-6605, 10.1039/C2CS35122F, 2012.